uOttawa

L'Université canadienne
Canada's university

FACULTÉ DES ÉTUDES SUPÉRIEURES ET POSTOCTORALES

uOttawa

L'Université canadienne
Canada's university

FACULTY OF GRADUATE AND POSDOCTORAL STUDIES

Lan Lin

AUTEUR DE LA THÈSE / AUTHOR OF THESIS

M.A.Sc. (Civil Engineering)

GRADE / DEGREE

Department of Civil Engineering

FACULTÉ, ÉCOLE, DÉPARTEMENT / FACULTY, SCHOOL, DEPARTMENT

Seismic Evaluation of the Confederation Bridge

TITRE DE LA THÈSE / TITLE OF THESIS

Nove Naumoski

DIRECTEUR (DIRECTRICE) DE LA THÈSE / THESIS SUPERVISOR

Murat Saatcioglu

CO-DIRECTEUR (CO-DIRECTRICE) DE LA THÈSE / THESIS CO-SUPERVISOR

EXAMINATEURS (EXAMINATRICES) DE LA THÈSE / THESIS EXAMINERS

David T. Lau

Beatriz Martin-Perez

Daniel Palermo

Gary W. Slater

LE DOYEN DE LA FACULTÉ DES ÉTUDES SUPÉRIEURES ET POSTDOCTORALES /
DEAN OF THE FACULTY OF GRADUATE AND POSTDOCORAL STUDIES

Seismic Evaluation of the Confederation Bridge

By

Lan Lin

Thesis submitted to the Faculty of the Graduate and Postdoctoral Studies
in partial fulfillment of the requirements for the M.A.Sc.degree
in Civil Engineering

Department of Civil Engineering
Faculty of Engineering
University of Ottawa

April 2005

Your file Votre référence
ISBN: 0-494-11327-8
Our file Notre référence
ISBN: 0-494-11327-8

Dedicated to my family,

Especially, my parents for their love and continuous support.

Acknowledgments

I wish to express my sincere gratitude to my supervisors Dr. Nove Naumoski and Dr. Murat Saatcioglu for their guidance and support during the course of this study.

I would like to thank Drs. Hiroshi Tanaka, Jag Humar, David Lau, and Heng Khoo for sharing their knowledge by offering the courses that helped me in this study.

Thanks and appreciation are due to Dr. John Adams and Mr. Stephen Halchuk of the Geological Survey of Canada for providing seismic hazard parameters for the Confederation Bridge.

My great acknowledgement is extended to the University of Ottawa for awarding admission scholarships.

Abstract

The 12.9 km Confederation Bridge, crossing the Northumberland Strait in eastern Canada, is one of the longest reinforced concrete bridges in the world. The bridge was designed for a service life of 100 years, which is twice the service life considered in the Canadian codes for highway bridges that were in use at the time. Much higher safety factors than those for typical highway bridges were used. In the design of the bridge, the seismic hazard was represented by a seismic design spectrum. This spectrum was derived by applying spectral amplification factors to the peak ground acceleration, velocity and displacement, corresponding to the design service life and the required safety of the bridge. The design forces and displacements due to seismic loads were computed using the response-spectrum analysis method.

This thesis presents results from a seismic evaluation study of the Confederation Bridge. The seismic hazard for the bridge location was represented by a uniform hazard spectrum corresponding to the most recent seismic source models of the surrounding regions. For the purpose of the seismic analysis of the bridge, a finite element model was developed using 3-D beam elements. The model was calibrated using measured data from static and dynamic tests of the bridge. A number of time-history analyses were conducted by applying seismic excitation motions representative of the seismic hazard of the location. The following seismic excitations were considered in the study: (i) excitations represented by the uniform hazard spectrum for the bridge location, (ii) ground motion records representative of seismic motions in eastern Canada, (iii) ground motion records representative of seismic motions from large earthquakes at large distances, (iv) records obtained during the 1988 Saguenay, Quebec earthquake, (v) records obtained during the 1982 Miramichi, New Brunswick earthquake, and (vi) simulated seismic ground motions for the bridge location. The bending moments and displacements obtained from the seismic analysis were compared with the design values. It was found that the seismic parameters used in the design are quite representative of the seismic hazard of the bridge location.

Table of Contents

List of Tables

List of Figures

Chapter 1

Introduction

1.1 Background

The Confederation Bridge, which was opened for traffic in June 1997, is 12,910 m long and is one of the longest reinforced concrete bridges built over water in the world. The bridge crosses the Northumberland Strait in eastern Canada and connects the province of Prince Edward Island and the province of New Brunswick.

The bridge is located in a region known for very harsh environmental conditions. The Strait is covered by ice approximately three to four months in a year. Heavy storms with winds in excess of 100 km/h are often experienced at the bridge site. Given the importance of the Confederation Bridge, its length, and the environmental conditions, special criteria were imposed in the design and construction of the bridge in order to provide a high degree of safety during its operational life. The bridge was designed for a service life of 100 years, which is twice the service life considered in the Canadian codes for highway bridges that were in use during the design of the Confederation Bridge, i.e., the CSA Standard CAN/CSA-S6-88 (CSA 1988), and the Ontario Highway Bridge Design Code (OHBDC) (MTO 1991). A safety index of 4.0 was used in the design, compared with 3.5 specified in CAN/CSA-S6-88 and OHBDC. Load combinations and load resistance factors were developed specifically for the design of the bridge, as described in MacGregor et al. (1997). A number of assumptions had to be made

in the design, particularly for the long-term properties of the materials in the specific environmental conditions and for the effects of various dynamic loads on the performance of the bridge. Given these assumptions, a comprehensive research program was undertaken to monitor and study the behaviour of the bridge. One of the major tasks of this program was the investigation of the behaviour of the bridge due to dynamic loads, including seismic, wind, traffic, and ice loads. This thesis presents results from a study on the performance of the bridge when subjected to seismic ground motions that might occur at the bridge location.

1.2 Objective and Scope of the Study

The main objective of this study is to evaluate the performance of the bridge when subjected to seismic excitations representative of seismic ground motions expected at the bridge location. To achieve this objective, the following research tasks were conducted in this study:

(i) Review of the seismic design parameters for the bridge.

(ii) Examination of the seismic hazard for the bridge location for a probability of exceedance corresponding to the design life of the bridge of 100 years and the design safety index of 4.0.

(iii) Comparison of the seismic design parameters with those from the new seismic hazard analyses.

(iv) Development of a finite element model of a typical three-span segment of the bridge using 3-D beam elements.

(v) Calibration of the finite element model using measured data from static and dynamic full scale tests on the bridge. This model was used for the seismic evaluation of the bridge and was referred to as the evaluation model.

(vi) Establishing a model similar to that used in the design of the bridge. This model was used for the estimation of the design response values, and was referred to as the design model.

(vii) Response-spectrum analysis of the design model for seismic actions represented by the design spectrum, to estimate the seismic response parameters used in the design of the bridge.

(viii) Response-spectrum analysis of the evaluation model for seismic actions represented by the uniform hazard spectrum for the bridge location.

(ix) Time-history analysis of the evaluation model using selected records representative of seismic ground motions in eastern Canada.

(x) Time-history analysis of the evaluation model using ground motion records obtained during the 1988 Saguenay, Quebec earthquake.

(xi) Time-history analysis of the evaluation model using ground motion records obtained during the 1982 Miramichi, New Brunswick earthquake.

(xii) Time-history analysis of the evaluation model using simulated seismic ground motions.

The seismic evaluation of the bridge was conducted by comparing the responses from the analyses in tasks (viii) to (xii) with the estimated design response values in task (vii).

1.3 Outline of the Thesis

The methods, the analyses, and the results from the analyses are described in five chapters. Chapter 2 presents a review of available literature related to this study. Chapter 3 discuses the seismic parameters used in the design of the bridge and the seismic hazard for the bridge location based on most recent hazard analyses. The development and the calibration of the finite element model for use in the analyses are described in Chapter 4. Chapter 5 discuses the seismic excitations, the dynamic analyses, and the responses obtained from the analyses. Comparisons of the computed responses with estimated design values are discussed in detail. Finally, Chapter 6 presents the main observations and conclusions resulting from the study. Recommendations for further research on the seismic performance of the bridge are also included.

Chapter 2

Literature Review

2.1 Seismic Design Criteria

The design criteria were specified by J. Muller International – Stanley Joint Venture Inc. (JMS 1996). A design service life of 100 years, and a design target safety index of 4.0 for multi-load path components, and 4.25 for single-load path components were prescribed in these criteria. The design criteria also prescribed the use of the response-spectrum method for determining the design forces and displacements of the bridge due to seismic effects. The horizontal and vertical seismic design spectra, as well as the peak ground acceleration, velocity, and displacement for the bridge location were given in this document.

Jaeger et al. (1997) described the seismic design parameters for the Confederation Bridge. Two approaches were used for the estimation of the peak ground motions at the bridge location. The first approach was based on probabilistic methods, and the second approach was based on engineering considerations. The peak ground motion values obtained by Jaeger et al. (1997) were 0.12 g for the acceleration, 10.8 cm/s for the velocity, and 5.9 cm for the displacement. These values were adopted for the design. The 5% damped elastic seismic design spectrum for horizontal seismic motions was developed using the foregoing values for the peak ground acceleration, velocity and displacement, and applying the corresponding spectral amplification factors proposed by Newmark and Hall (1982) for the mean plus one standard deviation level. Jaeger et al. (1997) also developed a finite element model for the bridge for use in the design. The elasticity of the foundation was not considered in the modelling (i.e. fixed base conditions were assumed).

2.2 Research Studies for the Bridge

Lau et al. (2004) presented results from a study on the dynamic modelling of the Confederation Bridge. Three models were developed using the computer program COSMOS. A 3-D model using shell elements and a frame model using 3-D beam elements were developed for one span of the bridge. The frame model was extended to include three consecutive spans. It was found that the natural frequencies of the first 10 modes of these three models were quite close. The three-span frame model was used to investigate the effects of the foundation flexibility on the natural frequencies of the modes. The model was calibrated using measured data from static and dynamic tests on the bridge. It was reported that the flexibility of the foundation lead to a reduction of the natural frequencies of some modes by approximately 12%. It was also concluded that the surrounding water had negligible effects on the natural frequencies.

Londono et al. (2004) reported results on the effects of the concrete temperatures on the dynamic properties of the Confederation Bridge. Natural frequencies were computed by analysing forty-two ensembles of records obtained over a period of 10 months. Each ensemble corresponded to a different concrete temperature within the range between -18°C to 25°C. For this range of temperatures, the variations of the natural frequencies relative to the average values were ±4.5%. As reported, this was due to changes of the material properties with temperature, in particular the modulus of elasticity of the concrete.

Brown and Croasdale (1997) described the static and dynamic pull tests conducted on the Confederation Bridge about two months before the official opening of the bridge. The tilts and the free vibrations measured during these tests were very valuable for the calibration of the finite element model developed in this study.

Ghali et al. (2000) reported measured data for the modulus of elasticity of the concrete of the Confederation Bridge. Measurements were taken at concrete age of 2, 7, 14, 28, 90 and 180 days. Based on these data, an equation was proposed for the prediction of the modulus of elasticity for a specified concrete age. This equation was used in this study for the estimation of the modulus of elasticity.

2.3 Seismic Motions for the Bridge Location

In addition to the foregoing publications related to the research on the bridge, of importance for this study was also the literature for the seismic hazard and the characteristics of seismic motions in eastern Canada. These issues were discussed in Adams and Halchuk (2003) and Adams and Atkinson (2003), and were essential for the selection of the seismic ground excitations for use in the analysis of the bridge. Also, Atkinson and Beresnev (1998) and Tremblay and Atkinson (2001) described a method for the simulation of seismic ground motions representative of the seismic hazard for a given location. Seismic motions simulated by Tremblay and Atkinson (2001) for eastern Canada were adapted for use in the evaluation of the bridge.

Chapter 3

Seismic Design Parameters and Seismic Hazard for the Confederation Bridge

3.1 Seismic Design Parameters for the Bridge

As discussed in the introductory chapter, the design life of 100 years and the safety index of 4.0 were the basic design requirements for the Confederation Bridge. These requirements were much higher than those prescribed in the highway bridge design codes available at the time. The specified design life and safety index for the Confederation Bridge required special studies in order to determine the seismic ground motion parameters at the bridge location.

The seismic ground motion parameters used in the design of the bridge were given in the design criteria specified by J. Muller International – Stanley Joint Venture Inc. (JMS 1996). These included the peak ground acceleration, the peak ground velocity, the peak ground displacement, and the seismic design spectrum for the bridge location. The methods for determining these parameters were described by Jaeger et al. (1997). Two methods were used for the estimation of the peak ground acceleration of the expected seismic motions at the bridge location. The first method was based entirely on probabilistic considerations. According to this method, the peak ground acceleration for the design service life of 100 years and the design safety index of 4.0 corresponded to an annual probability of exceedance of 0.00027. The value of the peak ground acceleration for this probability of exceedance was found to be A=0.136 g.

The second method was primarily based on engineering considerations. In this method, first, the peak ground acceleration was determined for a probability of exceedance

of 10% during the design service life of 100 years. The background for this was to keep the same probability of exceedance during the service life as that required by NBCC 1995. Then, the acceleration value corresponding to 10% in 100 years probability of exceedance was increased by applying a factor of 1.43 representing the product of the commonly used importance factor of 1.3, and an additional importance factor of 1.1 because of the unusual importance of the bridge. The resulting peak ground acceleration was 0.12 g, and this value was adopted for the design. Using the same approach, the peak ground velocity was found to be 10.8 cm/s. Having the values for the peak ground acceleration (A) and the peak ground velocity (V), a value for the peak ground displacement (D) of 5.9 cm was obtained using the relationship between A, V, and D, proposed by Newmark and Hall (1982).

The 5% damped elastic seismic design spectrum for horizontal seismic motions was developed using the foregoing values for the peak ground acceleration, velocity and displacement, and applying the corresponding spectral amplification factors proposed by Newmark and Hall (1982) for the mean plus one standard deviation level. This level corresponds to a probability of 84% that the spectral amplification factors will not be exceeded. The parameters for the construction of the horizontal design spectrum are given in Table 3.1, adopted from the design criteria. It can be seen that the spectrum was defined assuming a constant spectral acceleration in the short period range ($T < 0.5$ s), a constant spectral velocity in the intermediate period range ($0.5 \text{ s} < T < 3.0$ s), and a constant spectral displacement in the long period range ($T > 3.0$ s), which is a common approach for constructing design spectra based on peak ground motions and spectral amplification factors (Newmark and Hall 1982). The vertical design spectrum was taken as 2/3 of the horizontal spectrum (JMS 1996), which is also a common practice for defining vertical design spectra, based on the findings reported in Newmark et al. (1973).

Table 3.1 Parameters of the design spectrum for horizontal seismic motions; 5% damping (JMS 1996).

Period, T (s)	Governing parameter	Spectral acceleration (g)
< 0.5	Acceleration = 0.326 g	0.326
0.5 – 3.0	Velocity = 24.8 cm/s	0.1589 / T
> 3.0	Displacement = 11.8 cm	$0.48 / T^2$

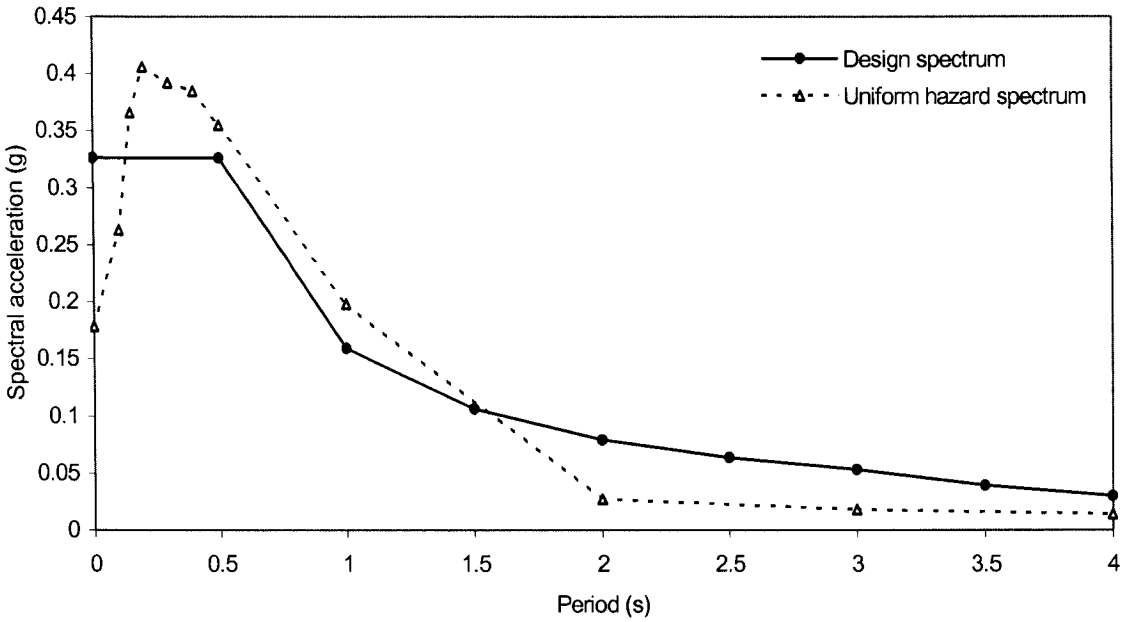

Figure 3.1 Design and uniform hazard spectra; 5% damping.

Figure 3.1 shows the horizontal seismic design spectrum. The other spectrum in the figure, designated "uniform hazard spectrum" is discussed below.

3.2 Seismic Hazard for the Bridge

Since the development of the design parameters for the Confederation Bridge in early 1990s, there have been significant advances in the understanding of the seismic hazard in Canada. New source models, and most updated software have been used for the assessment of the seismic hazard. It should be mentioned, however, that there are still significant uncertainties in the estimation of seismic hazard. As pointed out by Adams and Atkinson (2003), the ground motion attenuation relations for eastern Canada are the major source of uncertainty in the seismic hazard estimations. This is because of lack of recordings of ground motions from strong earthquakes in eastern Canada for use in the calibration of the attenuation relations. Given this, Adams and Atkinson (2003) noted that the ground motion attenuation relations for eastern Canada may change significantly as new events are recorded.

The seismic hazard is currently represented by uniform hazard spectra rather than by peak ground motions. A uniform hazard spectrum represents an acceleration spectrum with

spectral ordinates that have the same probability of exceedance. Uniform hazard spectra can be computed for different probabilities and confidence levels. Confidence levels of 50% (median) and 84% are typically used for uniform hazard spectra. These levels represent the confidence (in %) that the spectral values will not be exceeded for the specified probability.

For the purpose of this study, Geological Survey of Canada (GSC) computed the uniform hazard spectrum for the bridge location for an annual probability of exceedance of 0.00027 and confidence levels of 50% and 84%. Among the two confidence levels, the uniform hazard spectrum at the 84% confidence level was used in this study. The 84% (rather than 50%) level was chosen since the spectral amplification factors used in the development of the design spectrum are for that level. The 84% level uniform hazard spectrum (UHS) is shown in Fig. 3.1. The spectral values for periods below 2.0 s were provided by Geological Survey of Canada. For periods between 2.0 s and 4.0 s, the spectrum was extended assuming a constant spectral velocity with the same value as that at 2.0 s. This is the same as assumed in the defining of the spectral values in the intermediate period range of the design spectrum.

It can be seen from Fig. 3.1 that the uniform hazard spectrum is somewhat higher than the design spectrum for periods below 1.5 s. As will be discussed later, this difference does not have significant effects on the seismic response of the bridge.

3.3 Scenario Earthquakes for the Bridge

The seismic hazard at a given site represents the sum of the hazard contributions of different earthquakes at different distances from the site. For each site, however, there are a few earthquakes that have dominant contributions to the hazard. These earthquakes are normally referred to as scenario or predominant earthquakes. The shape of the uniform hazard spectrum for a given site, representing the seismic hazard for the site, depends on the magnitudes of the scenario earthquakes and the distances of these earthquakes from the site. In general, the dominant contribution to the short period ground motion hazard is from small to moderate earthquakes at small distances, whereas larger earthquakes at greater distance contribute most strongly to the long period ground motion hazard.

For the purpose of the selection of earthquake ground motions for use in the seismic analyses, it is necessary to determine the scenario earthquakes for the Confederation Bridge.

This can be done by computing the seismic hazard contributions of selected magnitude-distance ranges that cover all possible magnitude-distance combinations. Figure 3.2, provided by Geological Survey of Canada, shows the magnitude-distance contributions for the Confederation Bridge for annual probability of exceedance of 0.000404 (i.e. 2% in 50 years). Such graph could not be produced for a probability of exceedance of 0.00027 because of the uncertainties in the hazard analysis due to the extrapolations relative to the current hazard models. However, Tremblay and Atkinson (2001) reported that the predominant magnitude increases very slowly as probability decreases. Also, results reported in Halchuk and Adams (2004) indicated that the lowering of the probability has small effects on the predominant magnitude and distance values. Given this, the magnitude-distance contributions shown in Fig. 3.2 were considered to be representative of those for probability of exceedance of 0.00027.

Figure 3.2(a) shows the contributions to the seismic hazard for period of 0.2 s, representing the short period ground motion hazard. Similarly, Figure 3.2(b) shows the contributions for period of 2.0 s, representing the long period ground motion hazard. The contributions are computed for magnitude ranges of 0.25, and distance ranges of 20 km. It can be seen from Fig. 3.2(a) that the scenario earthquakes that have predominant contributions to the short period ground motion hazard are with magnitude ranging from 6 to 6.75 at distances of 60 km to 80 km. Similarly, Fig. 3.2(b) shows that the scenario earthquakes that have predominant contributions to the long period ground motion hazard are with magnitudes ranging from 7.25 to 7.5 at distances of approximately 500 km.

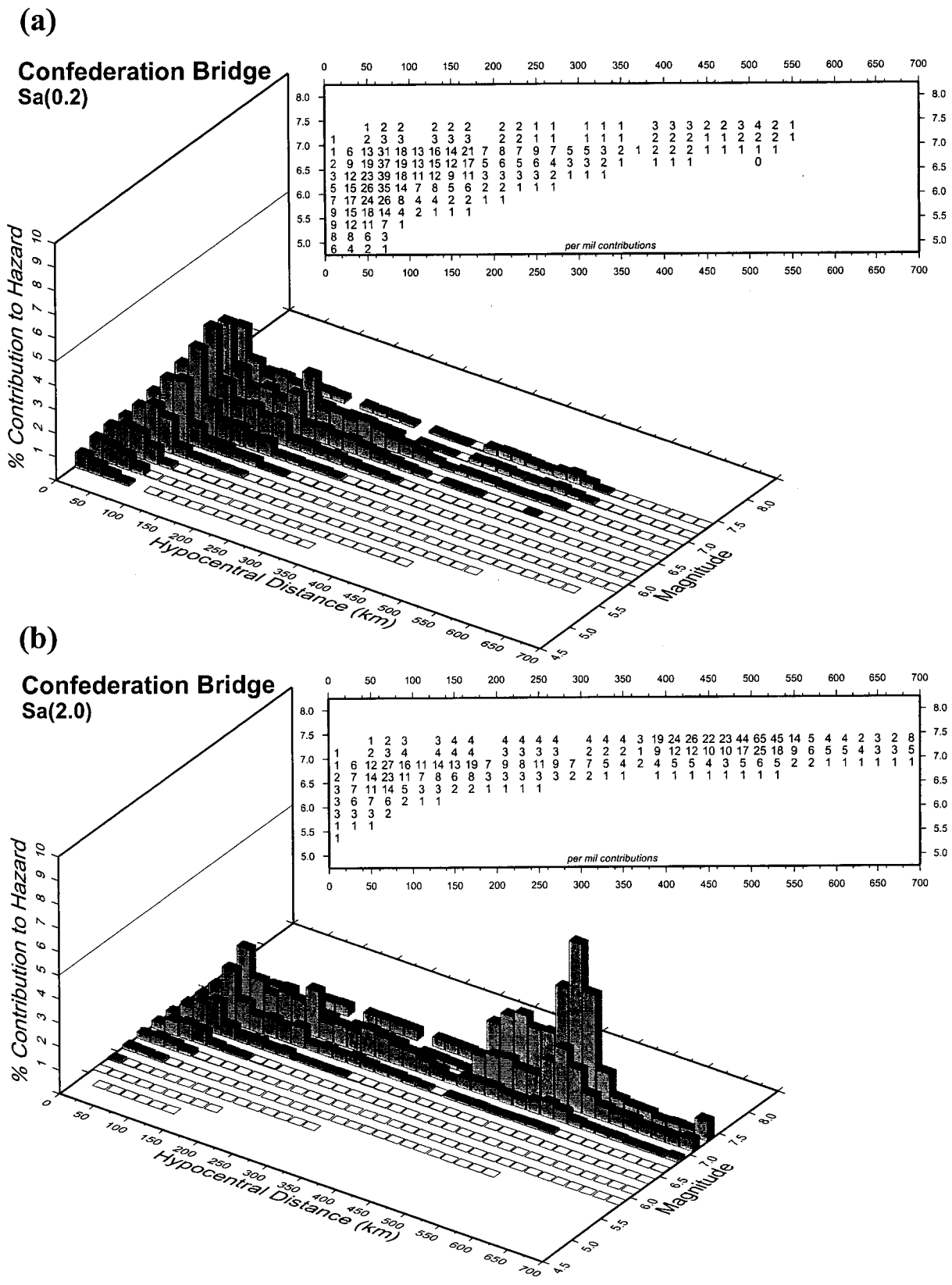

Figure 3.2 Magnitude-distance contributions to the seismic hazard of the Confederation Bridge, (a) for spectral acceleration at period of 0.2 s, and (b) for spectral acceleration at period of 2.0 s.

Chapter 4

Modelling of the Bridge

4.1 Description of the Bridge

The Confederation Bridge consists of two approach bridges at its ends and a main bridge between them (Fig. 4.1). The approach bridge at the Prince Edward Island end (i.e. the east end) is 555 m long and has 7 piers, and that at the New Brunswick end (i.e. the west end) is 1,275 m long and has 14 piers. The longest span of the approach bridges is 93 m. The main bridge is 11,080 m long and has 44 piers, designated P1 to P44 in Fig. 4.1. Of the 45 spans of the main bridge, 43 spans are 250 m long and the two end spans are 165 m long. The cross section of the bridge girder is a single-cell trapezoidal box. The depth of the girder of the main bridge varies from 4.5 m at mid spans to 14 m at piers. The width of the bridge deck is 11 m.

As shown in Fig. 4.1, the bridge deck of most of the main bridge is at elevation of 40.8 m above mean sea level (MSL). The height of the columns of this part of the bridge ranges from 38 to 62 m. In the middle portion of the main bridge, between piers P17 and P26, the elevation of the deck increases from 40.8 m at P17 and P26 to the highest elevation of 59.06 m at the central span P21-P22. This span is called the navigation span. The elevation of 59.06 m above MSL provides a 49 m vertical clearance for marine vessel traffic. The height of the piers of the navigation span is approximately 75 m.

Both the approach bridges and the main bridge were built of precast concrete segments

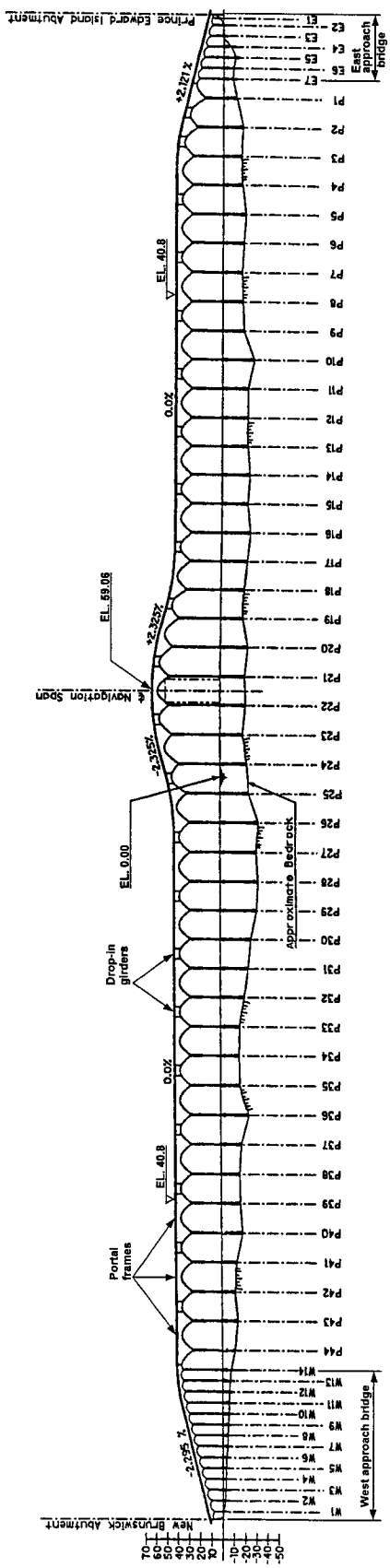

Figure 4.1 Elevation of the Confederation Bridge.

which were assembled using post-tensioned tendons. A detailed description of the bridge and the construction methods is given in Tadros (1997). Because this study is associated with typical spans of the main bridge, the discussion in the rest of this section will be focussed on structural features of the main bridge.

The structural system of the main bridge consists of a series of rigid portal frames connected by simply supported girders, which are called drop-in girders (Fig. 4.1). Every second span is constructed as a portal frame, and all other spans are constructed using drop-in girders. In total, there are 21 portal frames in the main bridge. This structural system was selected to prevent progressive collapse of the bridge due to extreme effects of wind, ice, seismic, and traffic loads, and ship collisions.

Figure 4.2 shows a typical portal frame of the main bridge. The girder consists of two 192.5 m double cantilevers and a 55 m long segment between them. The connections between this segment and the cantilevers are detailed to behave as rigid joints. The drop-in girders that connect the frames are also shown in Fig. 4.2, in the spans adjacent to the portal frame span. The length of the drop-in girders is 60 m. Each of the drop-in girders sits on the overhangs of the two adjacent portal frames. Four specially designed elastomeric bearings are used as supports. One of the bearings is fixed against translations and the remaining three allow translations of the girder only in the longitudinal direction. All four bearings allow rotations about all axes. This configuration of the bearings provides a hinge connection at one end, and longitudinal sliding connection at the other end of the drop-in girder.

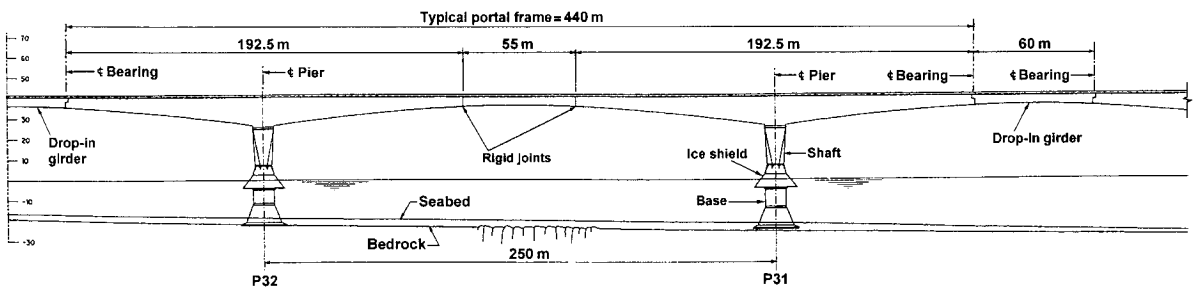

Figure 4.2 Typical portal frame.

The piers are constructed of two precast concrete units each, i.e. the pier base and the pier shaft (Fig. 4.2). The pier base is a hollow unit and has a circular cross section in plan with an outer diameter of 8 m at the top and 22 m at the footing. The pier shaft is also a hollow unit and consists of a shaft at the upper portion and an ice shield at the bottom portion of the pier. The cross section of the pier shaft varies from a rectangular section at the top to an octagonal section at the bottom of the shaft. Both the pier base and the pier shaft have very complex shapes. Detailed explanations for these and the geometrical properties of the piers can be found in Tadros (1997).

4.2 Modelling of the Bridge

The structural system of the bridge allows the development of a model of a selected segment of the bridge rather than modelling the entire bridge. Because of the repetitiveness of the units of the structural system (i.e. portal frames and drop-in girders) along the bridge, a proper model of a selected segment would be quite representative of the whole bridge.

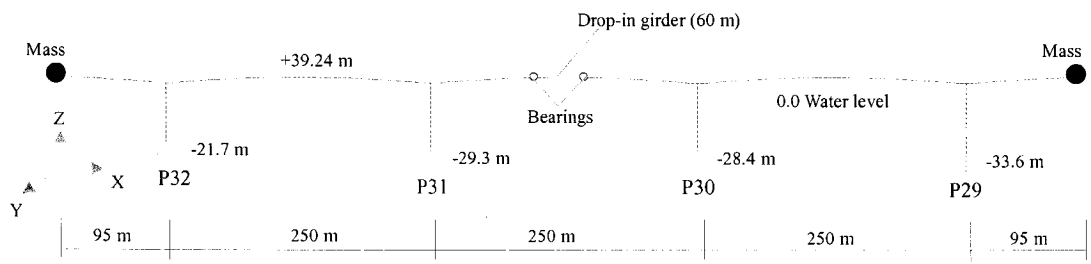

Figure 4.3 Model of two portal frames and one drop-in span using 3-D beam elements.

Figure 4.3 shows the finite element model used in this study. It is a three-span frame model consisting of 3-D beam elements. The modelling was conducted using the computer program SAP 2000 (Computers and Structures Inc. 2000). The model represents the bridge segment between piers P29 and P32 (Fig.4.1), which consists of two rigid portal frames (P29-P30 and P31-P32), and one drop-in span (P30-P31). This segment was modelled since it

is the instrumented portion of the bridge, and recorded data is available for use in the calibration of the model. The height of the piers of this segment is quite representative of the main bridge.

The model consists of 179 beam elements and 180 joints. The bridge girder is modelled by 123 elements, and each pier is modelled by 14 elements. The longitudinal axis (X) of the bridge is at the centroids of the cross section areas along the bridge girder. The geometrical properties of the end sections of the elements, such as cross-sectional area, moment of inertia, and torsional constant, were determined from the dimensions in the design drawings. Since the elements are non-prismatic, the variation of the bending stiffness along each element was taken into account in the modelling. These were based on the variations of the cross section dimensions along the elements. A cubic variation about the transverse axis (Y) and a linear variation about the vertical axis (Z) were used for the bending stiffness of the bridge girder elements, and a cubic variation of the stiffness about both the longitudinal and transverse axes of the cross sections were used for the pier elements.

The interaction with the adjacent drop-in girders (left of P32, and right of P29) was modelled by adding masses at the ends of the overhangs, as shown in Fig. 4.3. A half the mass of each drop-in girder was added at the end of the supporting overhang in transverse and vertical directions, full mass was added in the longitudinal direction for a hinge connection, and no mass was added in the longitudinal direction for a sliding connection. Similarly, vertical forces from a half the weight of each drop-in girder were applied at the ends of the overhangs.

In addition to the three-span model (Fig. 4.3), a single-span model consisting of a single portal frame (P31-P32), and a five-span model with three portal frames and two spans with drop-in girders (between P29 and P34; Fig. 4.1) were also considered. While the natural periods and mode shapes of these three models were quite comparable, the three-span model was chosen for the analysis in this study because it provides results for both the portal frame spans and the spans with drop-in girders, and requires an acceptable computation time for the

analysis. The single-span model does not provide results for the drop-in girder, and the five-span model requires an excessive computation time.

4.3 Calibration of the Model Using Data of Full Scale Tests

The model shown in Fig. 4.3 was calibrated using records of vibrations and tilts of the bridge obtained during a full scale tests of the bridge, that are referred to as pull tests. Also, measured data for the modulus of elasticity of the concrete were used in the calibration process. The measured data used, and the analysis conducted in the calibration of the model are discussed in detail hereafter.

4.3.1 Recorded Data During Pull Tests

Full scale pull tests were conducted on April 14, 1997, about two months before the official opening of the bridge. The objectives of the tests were: (i) to measure the deflection of the bridge pier under static loads, and (ii) to measure the free vibrations of the pier due to a sudden release of the static load. The instrumentation of the bridge (Fig. 4.4) was used to measure the bridge response during the pull tests. It consists of 76 accelerometers and 2 tiltmeters. The accelerometers were used to measure acceleration time histories of the response of the bridge. The two tiltmeters installed at locations 3 and 4 of pier P31 were used to measure the tilts of the pier.

The first pull test was a static test. Using a steel cable, a powerful ship pulled pier P31 in the transverse direction of the bridge. The pulling was at the top of the ice shield, approximately 6 m above the mean sea level. The force was increased steadily up to 1.43 MN, and then released slowly. The tilts at locations 3 and 4 were measured continuously during the test. The tilt at location 3 per unit applied force was 46.57 μR/MN, and that at location 4 was 42.99 μR/MN.

The second pull test was a dynamic test. In this test, the load was applied at a slow rate up to 1.40 MN and then suddenly released. This triggered free vibrations of the bridge, which were recorded by several accelerometers. Figure 4.5 shows the acceleration time history of the

transverse vibrations recorded at the middle of span P31-P32 (location 9 in Fig. 4.4). This record and those of the tilts were used in the calibration of the model.

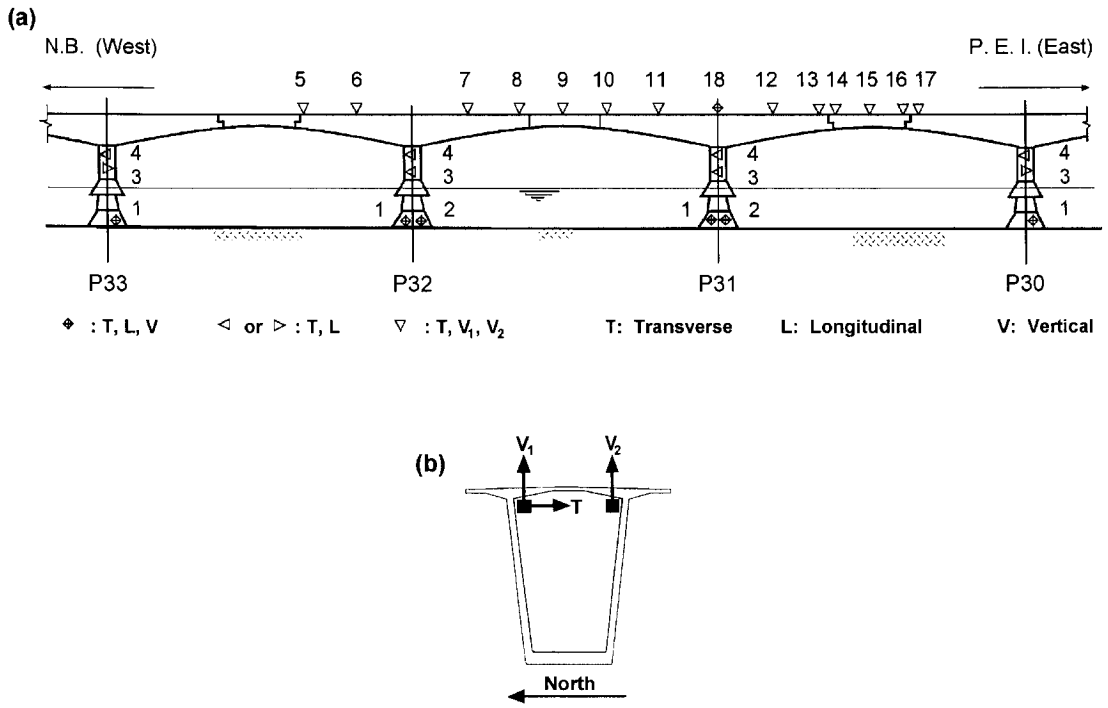

Figure 4.4 Locations of accelerometers: (a) instrumented sections of the bridge girder and piers, and (b) locations of accelerometers in the girder.

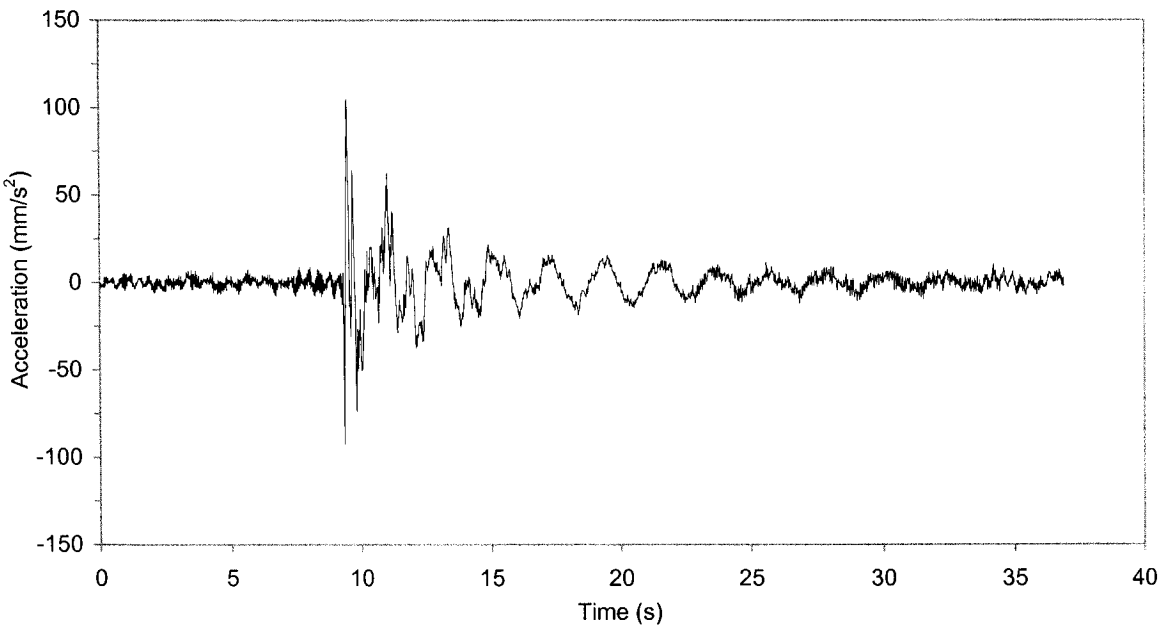

Figure 4.5 Acceleration time history of the transverse vibration at location 9.

4.3.2 Predominant Frequencies of the Recorded Vibrations

The predominant frequencies of the recorded vibrations were essential for the calibration of the model. These frequencies were determined using Fourier analysis. The Fourier amplitude spectrum of the vibration recorded at location 9 is shown in Fig. 4.6. Since the record consists of $N = 12{,}000$ acceleration data points at equal time intervals of $\Delta t = 0.0034$ s, the frequency resolution of the Fourier amplitude spectrum is $\Delta f = 0.0245$ Hz ($\Delta f = 1.0/(N \times \Delta t)$). From Fig. 4.6, it was found that the dominant frequencies of the vibration are $f_1 = 0.466$ Hz and $f_2 = 1.30$ Hz. These two frequencies were used in the calibration of the model.

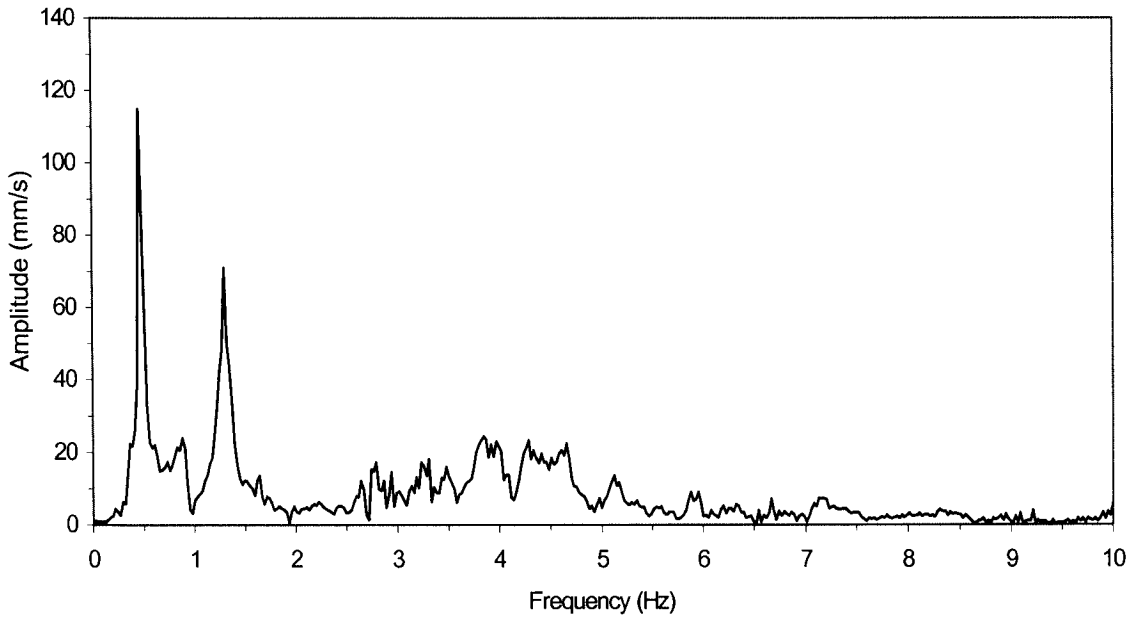

Figure 4.6 Fourier amplitude spectrum of the acceleration time history of the transverse vibration at location 9.

4.3.3 Damping Ratios of the Recorded Vibrations

In order to determine the damping ratios of the modes with frequencies of $f_1 = 0.466$ Hz and $f_2 = 1.30$ Hz, the time histories of the vibrations at these two frequencies were extracted from the record using numerical band-pass filters. In numerical filtering, it is important that the band-width of the filter is as wide as possible to avoid distortions of the time history, but at the same time to exclude effects of adjacent modes. In this study, a band from 0.346 Hz to 0.586 Hz was used to extract the modal vibrations at 0.466 Hz, and a band from 1.0 Hz to 1.5

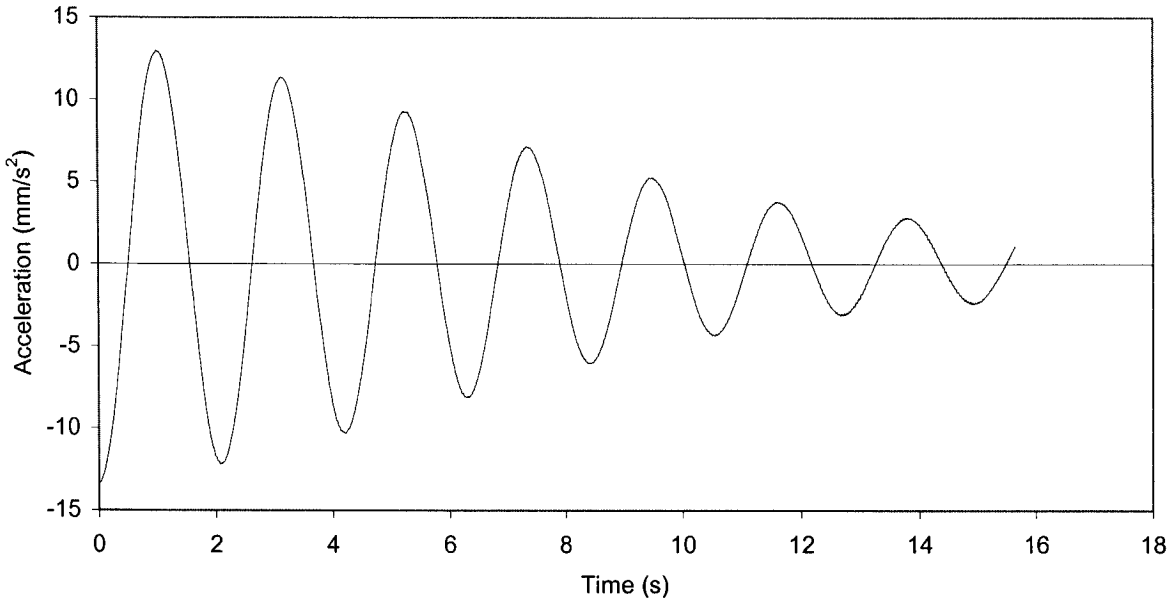

Figure 4.7 Band-pass (0.346 to 0.586 Hz) filtered acceleration time history of the transverse vibration at location 9.

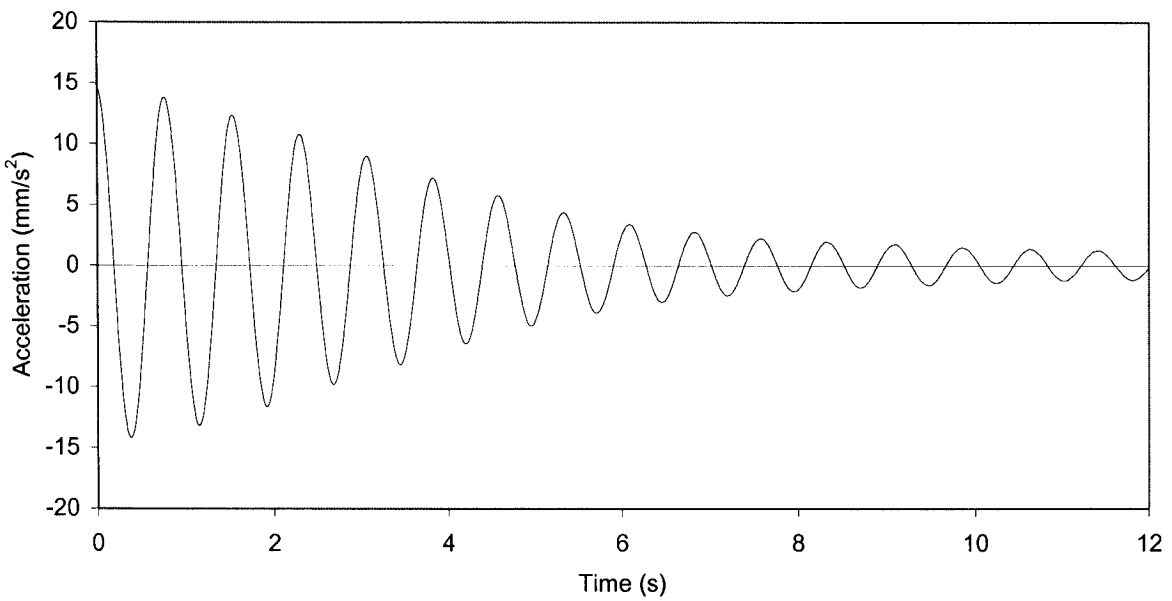

Figure 4.8 Band-pass (1.0 to 1.50 Hz) filtered acceleration time history of the transverse vibration at location 9.

Hz for the vibrations at 1.30 Hz. The extracted time histories are shown in Figs. 4.7 and 4.8. The damping ratios obtained from these time histories were ξ_1=0.038 for the modal vibrations at f_1=0.466 Hz, and ξ_2=0.032 for the vibrations at f_2=1.30 Hz. The average value of these two damping ratios is 0.035, and this value was used in the calibration of the model.

4.3.4 Modulus of Elasticity of the Concrete

During the construction of the bridge, cylinders were taken from the concrete used for the monitored part of the bridge between P31 and P32. The modulus of elasticity was measured at specified concrete age. Results from measurements at concrete age t = 2, 7, 14, 28, 90 and 180 days are reported in Ghali et al. (2000). Based on the measured data, Ghali et al. (2000) proposed the following equation for the prediction of the average modulus of elasticity of the concrete:

$$E_c(t) = E_c(28)\{\exp[s(1-(28/t)^{1/2})]\}^{1/2} \tag{4.1}$$

in which $E_c(t)$ is the elastic modulus at age t, $E_c(28)$ = 38.7 GPa is the average elastic modulus at age t = 28 days, and s = 0.25 is a coefficient for normal hardening cement assumed for the concrete used in the bridge.

Since the calibration of the model was based on the records obtained during the pull tests, Equation (4.1) was used to predict the modulus of elasticity at the time when the pull tests were conducted. Based on the information for the dates of the measurements reported in Ghali et al. (2000), it was found that the age of the concrete when the pull tests were conducted was approximately t = 60 days. For this concrete age, the average modulus of elasticity of 40,000 MPa was obtained using Equation (4.1). This value was used in the calibration of the model.

4.3.5 Calibration of the Model

The calibration was conducted using the model shown in Fig. 4.3. Since the calibration was based on measured data during the pull tests, it was important that the masses of the bridge

model correspond to those of the bridge during the pull tests. As reported by Brown and Croasdale (1997), the barriers and the pavement had not yet been in place at the time of the pull tests, and therefore the masses of these were not included in the calibration of the model. It is useful to mention that the masses of the pavement and the barriers are approximately 10% of the mass of the girder.

Given the available data described in Sections 4.3.1 to 4.3.4, the following parameters were used as reference parameters in the calibration of the model:

- Tilts at locations 3 and 4 of pier P31 recorded during the static pull test,
- Acceleration time history of the transverse vibrations at location 9 (Fig. 4.4) recorded during the dynamic pull test,
- Predominant frequencies of the recorded vibrations at location 9,
- Damping ratios of the predominant modes of the recorded vibrations, and
- Modulus of elasticity of the concrete of 40,000 MPa corresponding to the age of the concrete at the time when the pull tests were conducted.

The parameter that was varied in the calibration of the model was the foundation stiffness. While the soil under the foundations of the piers is designated "rock" in the design drawings, it is believed that there exist certain soil-structure interaction effects, and it is quite appropriate to consider these effects in the assessment of the dynamic behaviour of the bridge.

Rotational springs in the longitudinal and transverse directions were introduced in the model, at the bases of the piers, to represent the foundation stiffness. The calibration consisted of iterative performing the following sequence of tasks:

(i) The selection (in the first iteration), or the adjustment (in the subsequent iterations) of the rotational stiffness of the springs.

(ii) Static analysis of the model by applying a horizontal force of 1 MN to pier P31, 6 m above the mean sea level, in the transverse direction of the model.

(iii) Using the results from (ii), the tilts at locations 3 and 4 of pier P31 were computed, and

compared with the values measured during the static pull test.

(iv) Time-history analysis of the model by applying a loading representative of that used in the dynamic pull test. The loading was applied to pier P31, 6 m above the mean sea level, in the transverse direction of the model.

(v) Fourier analysis of the response time history of the model at location 9 (Fig. 4.4) to compute the Fourier amplitude spectrum. This spectrum was compared with that of the vibrations recorded at location 9 during the dynamic pull test.

Obviously, not always all the tasks were conducted in all iterations. For example, if the differences between the computed and measured tilts in task (iii) of a given iteration were larger than those in the previous iteration, then tasks (iv) and (v) were not proceeded, and a new iteration was undertaken.

For ease of understanding the calibration process, the main tasks of the process that include the comparison of the tilts (task (iii)), the time-history analysis of the model (task (iv)), and the comparison of the Fourier amplitude spectra (task (v)), are discussed in more details hereafter.

Comparison of Tilts

Results for the tilts of selected iterations of the calibration process are given in Table 4.1. The table shows the rotational stiffness used in the iterations and the corresponding tilts at locations 3 and 4 resulting from the static analysis of the model by applying a horizontal force of 1 MN to pier P31, 6 m above the mean sea level. For comparison, the tilts measured during the static pull test are also shown in the table. It can be seen that the stiffness of the foundation between 3.35 MN·m/μR and 4.45 MN·m/μR provides tilts that are quite close to the measured tilts. The differences between the computed and the measured tilts are smaller than 3%. Table 4.1 also shows that the computed tilts corresponding to fixed-base conditions are significantly smaller than the measured values. Obviously, this was expected since the bridge structure with rigid bases is stiffer than that with flexible bases.

Table 4.1 Foundation stiffness used in selected iterations and computed tilts at locations 3 and 4.

Foundation stiffness (MN·m/μR)	Computed tilts (in μR) and differences (in %) between computed and measured values			
	Location 3	Difference	Location 4	Difference
∞ (Fixed-bases)	34.78	-19.1[(1)]	38.15	-18.1
5.05	40.71	-5.3	44.72	-4.0
4.45	41.70	-3.0	45.54	-2.0
4.05	42.29	-1.6	46.36	-0.5
3.35	43.77	+1.8	48.00	+3.0
2.65	46.34	+7.8	50.67	+8.8
Measured values	42.99		46.59	

[(1)] Difference with negative sign indicates that the computed value is smaller than the measured value.

Time-history Analysis of the Model

For each foundation stiffness considered in the calibration process, a time-history analysis was conducted to compute the response time histories of the model. The loading used in the analysis was representative of that applied during the dynamic pull test. The load function is shown in Fig. 4.9. The load was assumed to increase linearly from 0 to 1.4 MN in 15 s, then it was kept constant for 10 s, and then was decreased linearly to zero in 0.13 s. The load was applied to pier P31, 6 m above the mean sea level, in the transverse direction of the model. The time-history analysis was conducted using a modal damping of 3.5%. A time interval of integration of 0.005 s was used in the time-history analysis.

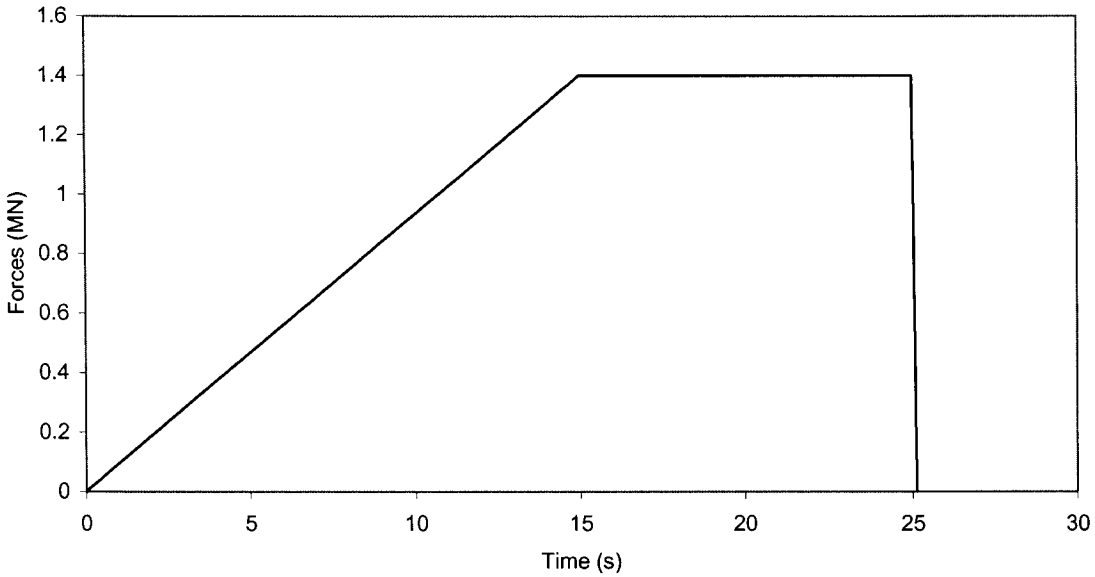

Figure 4.9 Load function for time-history analysis of the model.

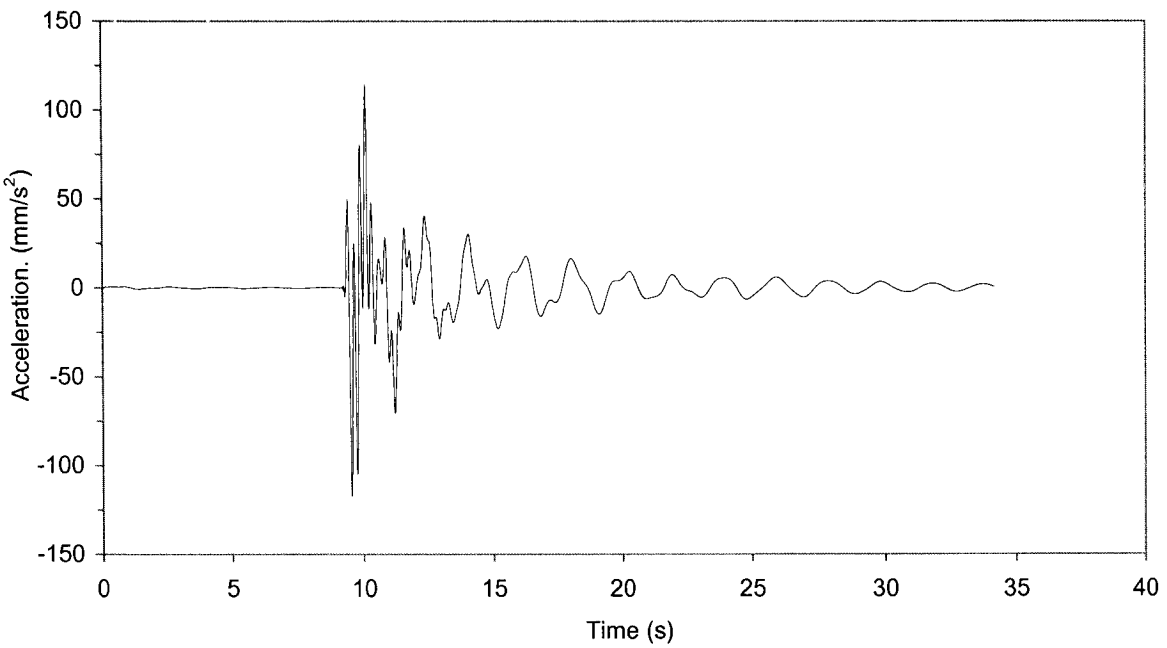

Figure 4.10 Computed acceleration time history of the transverse response at location 9.

Figure 4.10 shows the computed acceleration time history of the response of the bridge girder at location 9 (Fig. 4.4). Comparing this time history with the recorded vibration (Fig. 4.5), it can be seen that the computed response is in a good agreement with the measured response.

Comparison of Fourier Amplitude Spectra

For each foundation stiffness, Fourier amplitude spectrum was computed for the acceleration time history of the transverse response at location 9 obtained from the dynamic analysis. This spectrum was compared with the spectrum of the measured vibrations (Fig. 4.6). It was found that the foundation stiffness of 3.35 MN·m/μR provides a quite satisfactory match of the predominant frequencies of the computed and measured responses at location 9. Figure 4.11 shows the Fourier amplitude spectrum of the computed response for foundation stiffness of 3.35 MN·m/μR. It can be seen that this spectrum is quite close to that of the measured vibrations (Fig. 4.6). The first two predominant frequencies of the computed response are f_{r1} = 0.513 Hz and f_{r2} = 1.277 Hz, which are very close to the corresponding predominant frequencies of f_1 = 0.466 Hz and f_2 = 1.30 Hz of the measured vibration. It is useful to mention that the frequencies f_{r1} and f_{r2} correspond respectively to the 7^{th} and the 18^{th} modes of the model.

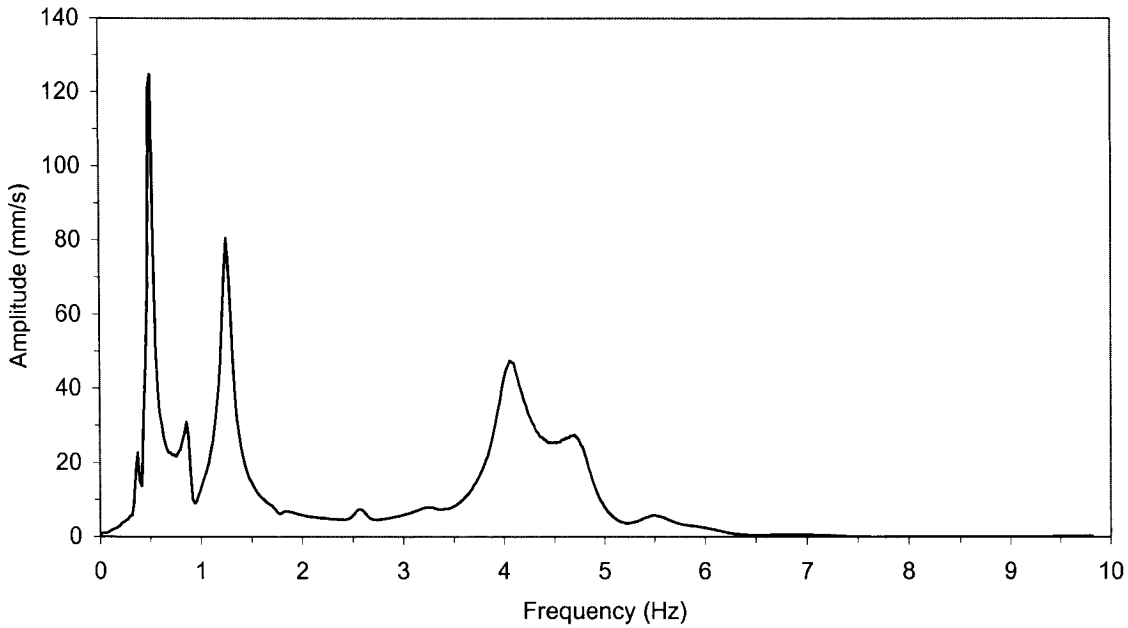

Figure 4.11 Fourier amplitude spectrum of the acceleration time history of the transverse response at location 9.

Based on the analyses of the Fourier amplitude spectra and those of the tilts, the foundation stiffness of 3.35 MN·m/μR was adopted to represent the foundation conditions of the bridge. This value was used in the further analyses in this study.

4.3.6 Parameters of the "Calibration Model" – Summary

The model established through the calibration process, described above, is referred to as the calibration model. This model was used as a reference model in this study. Based on the discussion on the development and the calibration of the model, the main parameters of the calibration model are as follows:

- Modulus of elasticity of the concrete, E_c = 40,000 MPa,
- Rotational stiffness of the foundation, K_{rf} = 3.35 MN·m/μR, and
- No masses of the barriers and the pavement are included in the model.

4.4 Evaluation Model

For the purpose of the seismic evaluation of the bridge, a new model was established, which was referred to as the evaluation model. The evaluation model has the same geometrical properties as those of the calibration model. The masses of the barriers and the pavement were included in the model. As was obtained in the calibration process, a foundation stiffness of 3.35 MN·m/μR was incorporated in the model. A modulus of elasticity of the concrete of 40,000 MPa was used as a reference value. Based on Equation (4.1), this represents an average modulus of elasticity for a concrete age of 60 days. As discussed in Chapter 5, values for the modulus of elasticity of 35,000 MPa and 43,700 MPa were also used to investigate the effects of the variations of the modulus of elasticity on the performance of the bridge.

4.5 Design Model

The seismic forces and displacements used in the design of the bridge were computed using a model developed by Jaeger et al. (1997). This model will be referred to as Jaeger's model. It is a 2-D frame model that was developed for the bridge segment between piers P2 and P6 (Fig. 4.1), which consists of two rigid frames (P3-P4 and P5-P6), and two drop-in spans (P2-P3 and P4-P5). The computer program SAP90 was used for the development of Jaeger's model. Since this model and the seismic design forces and displacements were not available, a model similar to Jaeger's model was developed to estimate the design values. This model was referred to as the design model. It has the same geometrical properties as the calibration model. The masses of the barriers and the pavement were included in the design model. As in Jaeger's model, fixed-base conditions were assumed for the design model. A modulus of elasticity of the concrete of 35,000 MPa was used for the design model, as specified in the design criteria (JMS 1996).

The natural periods and mode shapes of the design model were compared with those of Jaeger's model. The observations from the comparison are discussed in the next section.

4.6 Dynamic Characteristics of the Evaluation and Design Models

Since the seismic evaluation is based on the results from the analysis of the evaluation and the design models (see Chapter 5), it is useful to discuss the dynamic characteristics of these two models. Figure 4.12 shows the mode shapes and the corresponding natural periods of the first 10 modes of the evaluation model. The mode shapes of the first 10 modes of the design model are the same as those of the evaluation model. It can be seen from Fig. 4.12 that the 1st to the 5th mode, and the 7th mode represent transverse vibrations, the 6th and 8th modes represent combined vertical and longitudinal vibrations, and the 9th and the 10th modes represent vertical vibrations. It can be observed that the 1st, 2nd, 9th, and 10th modes consist almost exclusively of vibrations of the bridge girder and the vibrations of the piers are very small. The other modes of the model (i.e. the 3rd to the 8th mode) include vibrations of both the girder and the piers.

Figure 4.12 also illustrates that the vibrations of one of the rigid frames are dominant in the majority of the modes. For example, the vibrations of frame P29-P30 are dominant in the 1st, 4th, 5th, and the 6th mode, and the vibrations of frame P31-P32 are dominant in the 2nd, 7th and the 8th mode. This is because the connection between the frames is relatively week, and each frame may vibrate independently at its own frequency.

Table 4.2 shows the natural periods of the first 20 modes of the evaluation and the design models. Twenty modes were included in the table (rather than 10 modes shown in Fig. 4.12) in order to illustrate some features that were observed for the higher modes. As discussed earlier, the modulus of elasticity for the evaluation model is 40,000 MPa, and that for the design model is 35,000 MPa. Also, a rotational foundation stiffness is used for the evaluation model, and fixed-base conditions are assumed for the design model. As shown in Table 4.2, the natural periods of the first 10 modes of the design model are somewhat longer than those of the evaluation model. For the 11th to the 20th modes, the natural periods of the design model are shorter than those of the evaluation model. At first glance this observation is confusing, if only the foundation stiffness of the models is considered. However, the results can be

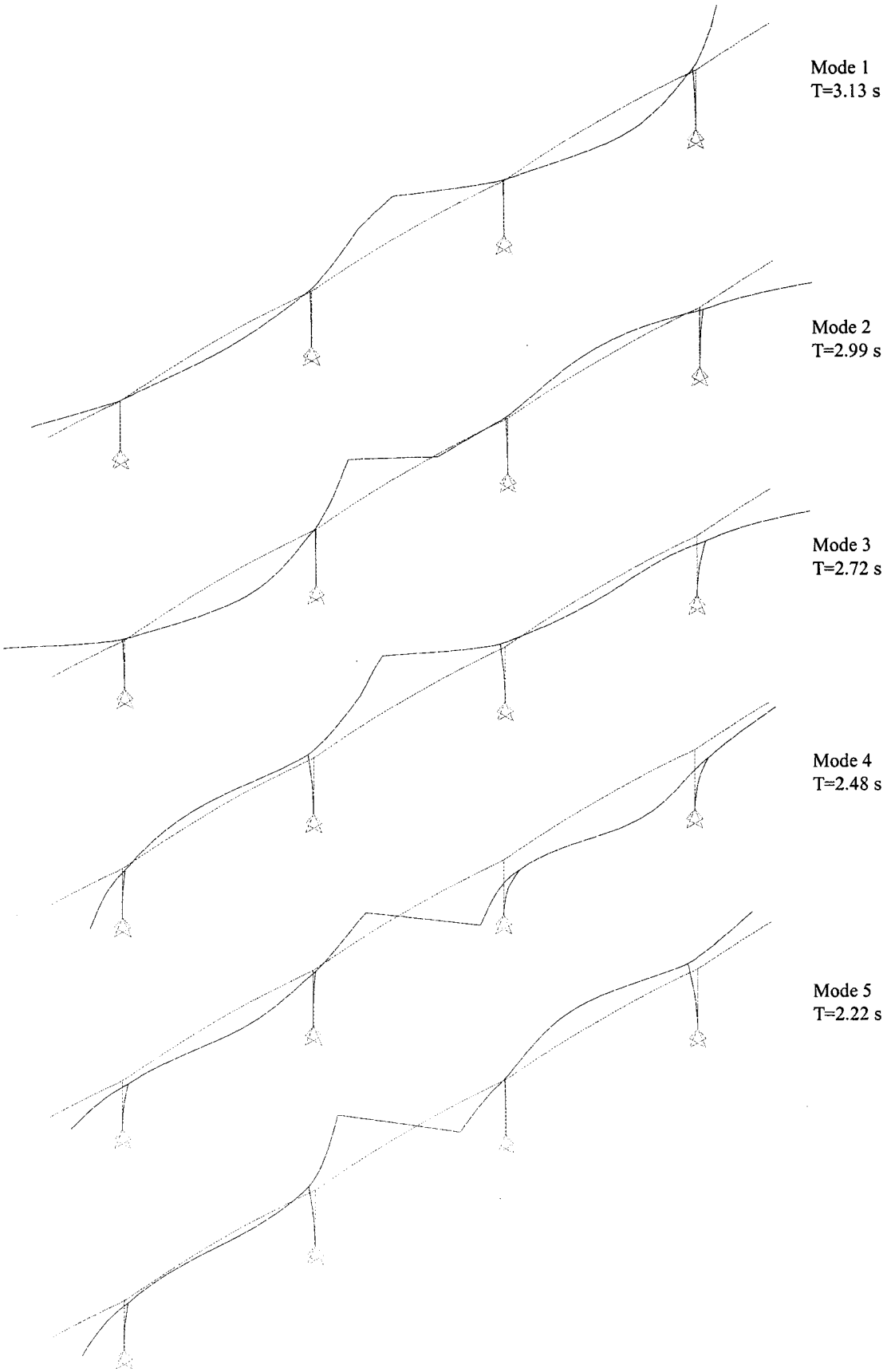

Figure 4.12 Mode shapes of the evaluation model.

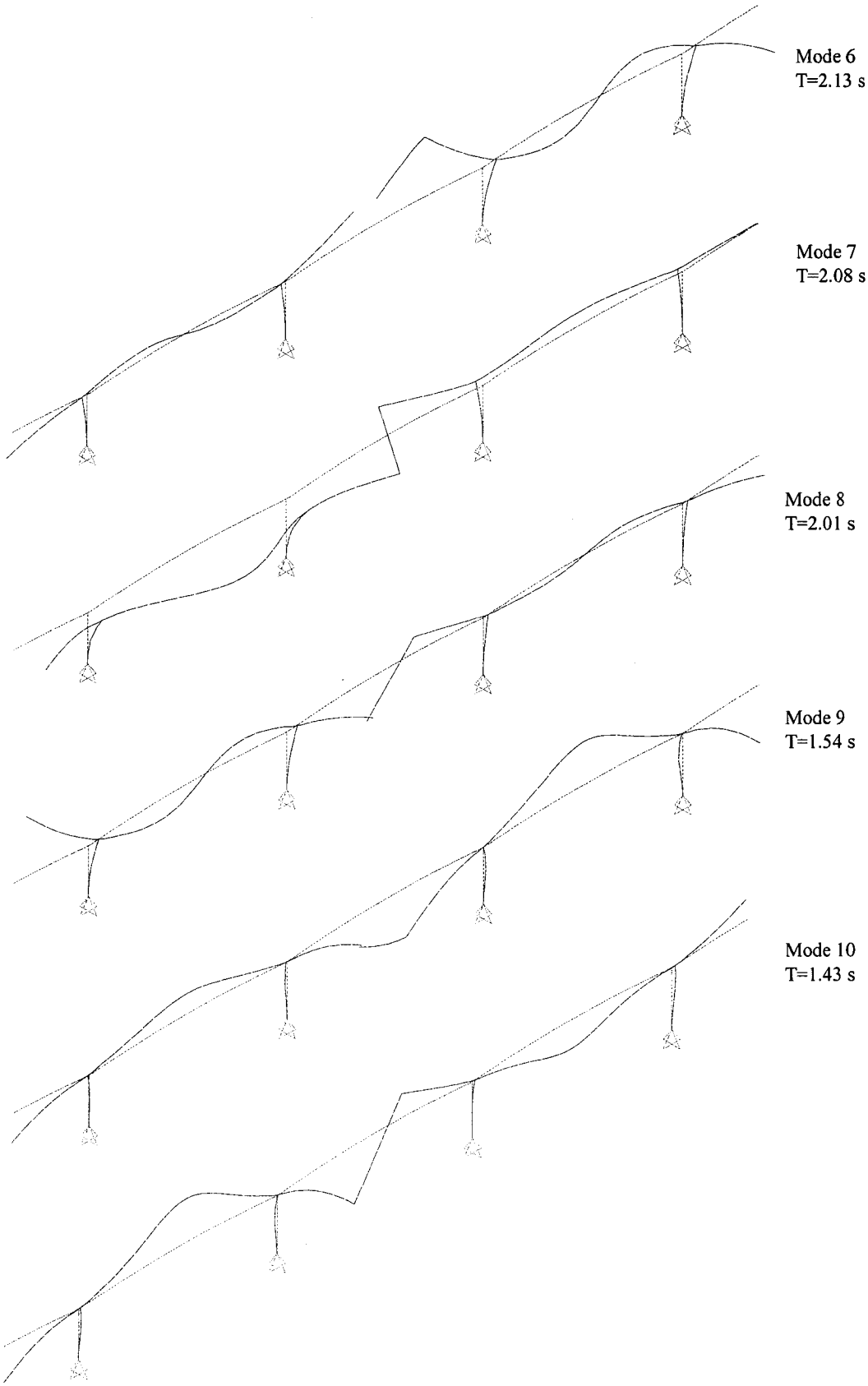

Figure 4.12 Mode shapes of the evaluation model (continued).

explained by considering the effects of both the foundation stiffness and the modulus of elasticity. In general, fixed-base conditions lead to shorter natural periods than those for flexible base conditions. On the other hand, modulus of elasticity of 35,000 MPa leads to longer natural periods than those for a modulus of elasticity of 40,000 MPa. The period values shown in Table 4.2 indicate that the difference in the modulus of elasticity of 5000 MPa has larger effects on the first 10 natural periods than the effects of the foundation stiffness used for the evaluation model.

Table 4.2 Natural periods of the first 20 modes of the evaluation and design models.

Mode No.	Natural periods (s)		
	Evaluation model E_c=40,000MPa	Design model E_c=35,000MPa	Variation of design model E_c=40,000MPa
1	3.128 T[(1)]	3.338 T	3.125 T
2	2.994 T	3.192 T	2.985 T
3	2.719 T	2.849 T	2.667 T
4	2.480 T	2.593 T	2.427 T
5	2.221 T	2.270 T	2.123 T
6	2.132 V, L	2.215 V, L	2.070 V, L
7	2.081 T	2.121 T	1.984 T
8	2.010 V, L	2.087 V, L	1.953 V, L
9	1.537 V	1.603 V	1.499 V
10	1.425 V	1.480 V	1.385 V
11	1.374 T	1.313 T	1.228 T
12	1.261 T[(2)]	1.205 V[(3)]	1.127 V
13	1.209 V[(3)]	1.202 T[(2)]	1.124 T
14	1.165 V, L	1.160 V, L	1.085 V, L
15	1.026 V, L	0.976 V, L	0.913 V, L
16	0.942 T	0.913 T	0.854 T
17	0.926 V, L	0.882 V, L	0.825 V, L
18	0.883 T	0.851 T	0.796 T
19	0.644 T	0.638 T	0.597 T
20	0.631 V, L	0.618 V, L	0.578 V, L

[(1)] T = transverse mode, V = vertical mode, V, L = combined vertical and longitudinal mode.
[(2)] The shape of the 12th mode of the evaluation model is the same as that of the 13th mode of the design model.
[(3)] The shape of the 13th mode of the evaluation model is the same as that of the 12th mode of the design model.

To illustrate the effects of the foundation stiffness on the natural periods, Table 4.2 also includes the periods of a new model, designated "variation of design model", which is the same as the design model but with a modulus of elasticity of 40,000 MPa. The mode shapes of the new model are the same as those of the evaluation model. The effects of the foundation stiffness on the natural periods can be determined by comparing the period values of the new model with those of the evaluation model. As expected, the natural periods of the new model are shorter than those of the evaluation model. The difference between the periods is larger for the higher modes. The largest difference of 12% is for the 11^{th} mode.

Table 4.3 Comparison of natural periods of design and Jaeger's models.

Natural periods, T (s)			
Mode No.[1]	Design model	Jaeger's model	$T_{design}/T_{Jaeger's}$
1	3.338 T[2]	3.362 T	0.99
2	3.192 T	3.294 (3.101)[3] T	0.97 (1.03)
3	2.849 T	2.858 T	1.00
4	2.593 T	2.332 T	1.11
5	2.270 T	2.664 T	0.85
6	2.215 V,L	2.307 V,L	0.96
7	2.121 T	2.257 T	0.94
8	2.087 V,L	2.193 V,L	0.95
9	1.603 V	[4]	
10	1.480 V	[4]	

[1] Mode No. corresponds to modes of design model.
[2] T = transverse mode, V = vertical mode, V, L = combined vertical and longitudinal mode.
[3],[4] See discussion.

It is of special importance to compare the natural periods of the design model used in this study and those of Jaeger's model (see Section 4.5). Table 4.3 shows the natural periods of the design model and those of the corresponding modes of Jaeger's model. Note that only the first 10 modes are available for Jaeger's model (Jaeger et al. 1997). One of the modes is a local mode of the double cantilever at pier P2 (see Fig. 4.1), and this is specific only for Jaeger's model. Among the remaining 9 modes of Jaeger's model, seven modes have the same shapes

as those of the design model, and two modes have very similar shapes to the second mode shape of the design model. The periods of these two modes of 3.294 s and 3.101 s are also very close to the period of 3.192 s of the second mode of the design model (see Table 4.3). The ratios of the modal periods of the design model to those of Jaeger's model ($T_{design}/T_{Jaeger's}$) are also shown in Table 4.3. It can be seen that the largest differences of 11% and 15% are for the 4^{th} and the 5^{th} modes respectively, and the differences for all other modes are less than 6%. Given this, the design model developed in this study was considered to be quite appropriate for the estimation of the design values.

Chapter 5

Analysis and Results

5.1 Overview of Analyses

To investigate the performance of the bridge due to seismic loads, a number of dynamic analyses were conducted using the evaluation model. The computer program SAP 2000 (Computers and Structures Inc. 2000) was used for the analyses. The seismic evaluation of the bridge was conducted by comparing the results from the analyses of the evaluation model with estimated design values using the design model. The analyses carried out in this study, in the order as performed, are the following:

(i) Time-history analysis of the evaluation model to investigate the effects of the modulus of elasticity of the concrete on the response parameters.

(ii) Response-spectrum analysis of the design model for seismic actions represented by the design spectrum. This analysis was conducted to estimate the seismic response parameters used in the design of the bridge.

(iii) Response-spectrum analysis of the evaluation model for seismic actions represented by the uniform hazard spectrum for the bridge location.

(iv) Time-history analysis of the evaluation model using selected records representative of seismic ground motions in eastern Canada.

(v) Time-history analysis of the evaluation model using ground motion records obtained

during the 1988 Saguenay, Quebec earthquake.

(vi) Time-history analysis of the evaluation model using ground motion records obtained during the 1982 Miramichi, New Brunswick earthquake.

(vii) Time-history analysis of the evaluation model using simulated seismic ground motions for eastern Canada.

It can be seen that two of the analyses are response-spectrum analyses, and all the others are time-history analyses. In general, response-spectrum analysis is simpler and less time consuming than time-history analysis, and consequently, the response parameters resulting from spectrum analyses are quite limited compared with those from time-history analysis. Response-spectrum analysis provides approximate estimates of the response maxima, and time-history analysis provides an accurate and detailed representation of the seismic performance of the structure for the specified seismic excitations and structural parameters. Given this, the time-history analysis was the primary method for the seismic evaluation of the bridge. The response-spectrum analyses, in items (ii) and (iii) above, were employed because the seismic actions in these two cases were defined by ground motion spectra. Since the analysis methods were of primary importance in the seismic evaluation of the bridge, the main features of the response-spectrum analysis and the time-history analysis, and the parameters used in these analyses that were specific for this study are described in the next section.

5.2 Description of Analyses

5.2.1 Response-Spectrum Analysis

Separate response-spectrum analyses were conducted for the following two cases of seismic actions: (i) seismic actions in the longitudinal and vertical directions of the bridge, and (ii) seismic actions in the transverse and vertical directions. In each of these cases, the horizontal and the vertical excitations were assumed to act simultaneously. The seismic actions were represented by 5% damped horizontal and vertical spectra. The analyses included the first

100 modes. The response maxima at each joint of the model were computed by combining the modal responses using the complete quadratic combination (CQC) rule.

5.2.2 Time-History Analysis

As in the response-spectrum analysis, time-history analyses were conducted for simultaneous seismic excitations in the longitudinal and vertical directions of the bridge, and in the transverse and vertical directions. In each analysis, the seismic excitations consisted of a pair of scaled horizontal and vertical acceleration time histories, applied at the bases of the piers. For simplicity, however, in most cases the excitations were referred to as excitations in the "longitudinal" or "transverse" direction, depending on the direction of the horizontal excitations. The horizontal time history of each pair was scaled to the median peak ground velocity of 7.1 cm/s, provided by Geological Survey of Canada for an annual probability of exceedance of 0.00027 (see Chapter 3), and the vertical time history was multiplied by the same scaling factor. Scaling to peak ground velocity is quite appropriate for this study because the predominant periods of the bridge are in the velocity controlled region, i.e. approximately between 0.5 s and 3.5 s.

Elastic material properties were assumed in the time-history analyses. The step-by-step numerical integration method was used. All the analyses were conducted using a time interval of integration of 0.005 s, and a 5% damping.

5.3 Description and Presentation of Response Parameters

The response parameters provided by both the response-spectrum analysis and the time-history analysis included bending moments, shear forces, axial forces, and displacements. A detailed review of the response parameters showed that the bending moments and the displacements are quite sufficient for representing the seismic performance of the bridge. The observations from the shear forces and the axial forces are the same as those from the bending moments. Given this, the bending moments and the displacements were used for the evaluation of the seismic performance of the bridge.

To assist in understanding the results from the analyses, it is useful to describe the convention for the moments and displacements, as used in this study. In reference to the coordinate system shown in Fig. 4.3, longitudinal moments in the bridge girder are those that act in the vertical plane X-Z, and transverse moments are those that act in the horizontal plane X-Y. For the piers, the moments that result from longitudinal excitations and act in the X-Z plane are referred to as "moments in the longitudinal direction", and those that result from transverse excitations and act in the Y-Z plane are referred to as "moments in the transverse direction". Positive longitudinal moments in the bridge girder act counter-clockwise about Y-axis, and positive transverse moments act clockwise about the Z-axis. For the piers, positive moments in the longitudinal direction act counter-clockwise about Y-axis, and positive moments in the transverse direction act clockwise about X-axis. Regarding the displacements, the positive longitudinal, transverse, and vertical displacements are in the directions of the positive X, Y, and Z-axes respectively.

The moments and the displacements at the joints of the model resulting from the response-spectrum analysis represent the maximum absolute values and by definition are positive. The time-history analysis provided a comprehensive set of results for each excitation. Time histories, maximum positive and negative values of the moments and displacements were obtained for each joint of the model. *Positive* moment and displacement envelopes for both the girder and the piers were plotted by using the *absolute* values of the computed (positive and negative) maxima. These envelopes represented the maximum positive moments and displacements resulting from reversible excitations, i.e. from separate actions of the seismic excitations in the positive and in the negative directions (see Fig. 4.3). The negative envelopes are a mirror image of the positive envelopes with respect to the longitudinal axes of the structural members considered.

The positive moment envelopes for the bridge girder were plotted using the values for 31 sections along the girder. These were selected to depict the variation of the moments along the bridge girder. Similarly, positive moment envelopes for each pier were plotted using the

values for 6 selected sections. The observations from the envelopes of the four piers were quite similar, and therefore, only the envelopes of pier P31 are presented. Regarding the displacements, envelope values are presented for 11 characteristic sections of the bridge girder.

5.4 Effects of Modulus of Elasticity of Concrete on Natural Periods

As discussed in Chapter 4, the modulus of elasticity of the concrete of the design model was 35,000 MPa, and that of the evaluation model was 40,000 MPa. It is known that the modulus of elasticity varies with the age and the temperature of the concrete. Given this, it was important to investigate the effects of the variation of the modulus of elasticity on the natural vibration periods. The natural periods of the evaluation model were computed for modulus of elasticity of the concrete, E_c, of 35,000 MPa, 40,000 MPa, and 43,700 MPa. The value of 43,700 MPa was computed using Equation (4.1) and represents the maximum modulus of elasticity of the concrete. The values of 35,000 MPa and 43,700 MPa represent estimates for the lower and upper bounds of the modulus of elasticity of the bridge, and the value of 40,000 MPa also represents an approximation for the average modulus of elasticity.

Table 5.1 shows the natural periods of the first 20 modes corresponding to the foregoing values for the modulus of elasticity. The periods designated T_{35000}, T_{40000}, and T_{43700} correspond respectively to E_c=35,000 MPa, E_c=40,000 MPa, and E_c=43,700 MPa. As expected, the longest periods are those for E_c=35,000 MPa (i.e. for the flexible model), and the shortest periods are those for E_c=43,700 MPa (i.e. for the stiffest model). The variations of the period values relative to the values corresponding to E_c=40,000 MPa are expressed by the ratios T_{35000}/T_{40000} and T_{40000}/T_{43700}. It can be seen that the periods for E_c=35,000 MPa are approximately 6.5% larger than those for E_c=40,000 MPa, and the periods for E_c=40,000 MPa are approximately 4.5% larger than those for E_c=43,700 MPa. In other words, the variation of the modulus of elasticity of the concrete between E_c=35,000 MPa and E_c=43,700 MPa can cause a total variation of the periods of approximately 11% relative to the average periods for this range of elasticity moduli. It is interesting to note that a similar variation of the periods has

been observed as a result of the variation of the temperature of the concrete (Londono et al. 2004). Based on measured records on the Confederation Bridge, Londono et al. (2004) reported that the variation of the average concrete temperature between –18°C and 25°C can cause a total variation of the natural periods of 9% relative to the average periods.

Table 5.1 Natural periods of the evaluation model for modulus of elasticity values of 35,000 MPa, 40,000 MPa, and 43,700 MPa.

Mode No.	Period, T (s)			Ratios	
	T_{35000} [(1)]	T_{40000} [(2)]	T_{43700} [(3)]	T_{35000}/T_{40000}	T_{40000}/T_{43700}
1	3.343	3.128	2.993	1.069	1.045
2	3.199	2.994	2.865	1.068	1.045
3	2.900	2.719	2.606	1.067	1.043
4	2.644	2.480	2.378	1.066	1.043
5	2.362	2.221	2.133	1.063	1.041
6	2.271	2.132	2.045	1.065	1.043
7	2.211	2.081	1.999	1.062	1.041
8	2.141	2.010	1.928	1.065	1.043
9	1.639	1.537	1.473	1.066	1.043
10	1.519	1.425	1.366	1.066	1.043
11	1.374	1.292	1.242	1.063	1.040
12	1.261	1.187	1.141	1.062	1.040
13	1.209	1.131	1.083	1.069	1.044
14	1.165	1.091	1.044	1.068	1.045
15	1.026	0.966	0.928	1.062	1.041
16	0.942	0.884	0.849	1.066	1.041
17	0.926	0.871	0.837	1.063	1.041
18	0.884	0.830	0.797	1.065	1.041
19	0.644	0.603	0.577	1.068	1.045
20	0.631	0.592	0.567	1.066	1.044

[(1), (2), (3)] Periods for modulus of elasticity of 35,000 MPa, 40,000 MPa, and 43,700 MPa respectively.

5.5 Effects of Modulus of Elasticity of Concrete on Response Parameters

As for the periods, the effects of the modulus of elasticity of the concrete on the response of the bridge was investigated by analyzing the evaluation model using modulus values of 35,000 MPa, 40,000 MPa, and 43,700 MPa. Several time-history analyses were conducted by subjecting the model to different seismic excitations. The results presented in this section were obtained from an analysis using excitations represented by ground motion

records obtained during the 1988 Saguenay, Quebec earthquake. Specifically, the horizontal and vertical acceleration time histories of record No. 5 in Table 5.7 were used in the analyses. The horizontal time history was scaled to the peak ground velocity for the bridge location of 7.1 cm/s, and the scaling factor obtained was applied to the vertical time history. Regarding the effects of the modulus of elasticity on the response parameters, the results for this excitation are representative of those for the other excitation motions.

The envelopes of the positive longitudinal moments in the bridge girder for excitation motions in the longitudinal direction are shown in Fig. 5.1(a), and those of the positive transverse moments for excitation motions in the transverse direction are shown in Fig. 5.1(b). It should be mentioned that the values for the moments at the joints at the piers (designated P29, P30, P31, and P32 in the figures) represent the average values of the moments of the beam members at the left- and right-hand sides of the joints.

The positive moment envelopes for pier P31 for excitations in the longitudinal and transverse directions are shown in Figs. 5.2(a) and 5.2(b) respectively. As can be seen from Figs. 5.1 and 5.2, the envelopes corresponding to the three values of the modulus of elasticity are quite close. The envelopes for E_c=40,000 MPa are between those for E_c=35,000 MPa and Ec=43,700 MPa at the majority of the sections. A simple statistics showed that the average variation of the moment envelopes for E_c=35,000 MPa and E_c=43,700 MPa relative to those for E_c=40,000 MPa was ±6.5% for the longitudinal moments in the girder, ±7.5% for the transverse moments in the girder, and ±8.5% for the moments in both the longitudinal and transverse directions of pier P31.

Table 5.2 shows the maximum values of the vertical and transverse displacements at selected sections of the bridge girder for excitations in the longitudinal and transverse directions. As for the moments, the displacements obtained for E_c=40,000 MPa are between those for E_c=35,000 MPa and E_c=43,700 MPa at most of the sections. The average variation of the displacements for E_c=35,000 MPa and E_c=43,700 MPa relative to those for E_c=40,000 MPa was approximately ±6% for the vertical displacements and ±8% for the transverse

displacements.

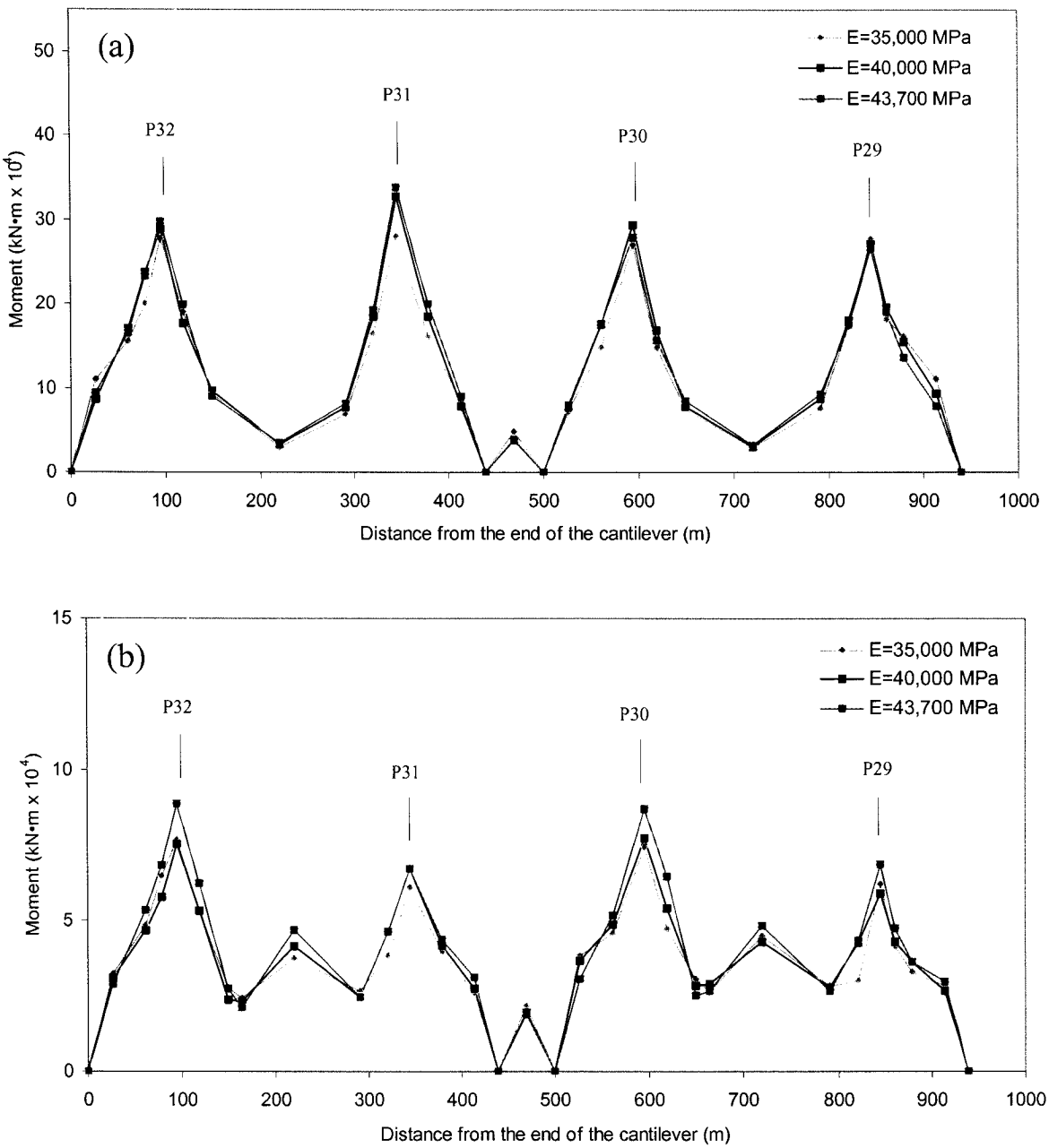

Figure 5.1 Envelopes of positive moments in the bridge girder for modulus of elasticity values of 35,000 MPa, 40,000 MPa, and 43,700 MPa, (a) Longitudinal moments, (b) Transverse moments.

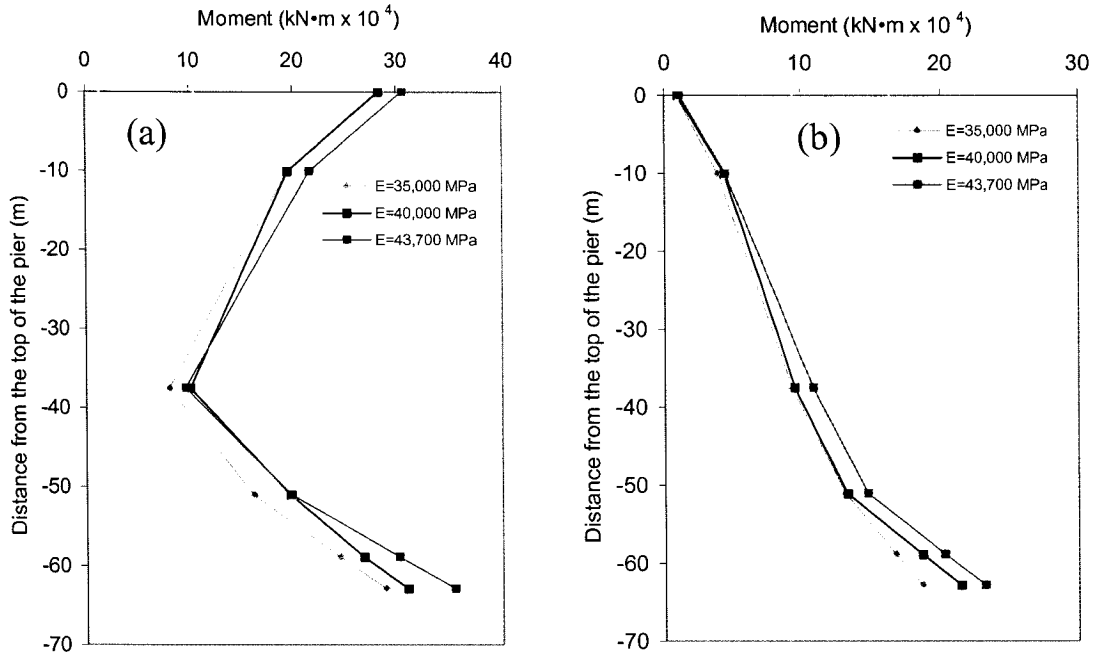

Figure 5.2 Envelopes of positive moments in pier P31 for modulus of elasticity values of 35,000 MPa, 40,000 MPa, and 43,700 MPa, (a) In longitudinal direction, (b) In transverse direction.

Table 5.2 Maximum vertical and transverse displacements of the bridge girder for modulus of elasticity values of 35,000 MPa, 40,000MPa, and 43,700 MPa.

Location	Vertical displacement (mm)			Transverse displacement (mm)		
	$d_{v,35000}$ [2]	$d_{v,40000}$ [3]	$d_{v,43700}$ [4]	$d_{t,35000}$ [5]	$d_{t,40000}$ [6]	$d_{t,43700}$ [7]
End of cantilv., left of P32[1]	77	68	66	43	48	51
Pier P32	0	0	0	19	18	21
Mid-span (P31-P32)	43	40	40	49	59	61
Pier P31	0	0	0	22	19	20
Bearing (left)	79	79	78	34	30	31
Middle of drop-in girder	43	38	37	32	34	39
Bearing (right)	79	88	78	45	49	56
Pier P30	0	0	0	24	22	22
Mid-span (P29-P30)	41	39	39	56	55	65
Pier P29	0	0	0	26	24	23
End of cantilv., right of P29	76	63	58	34	33	36

[1] See Figure 4.3 in Chapter 4; applies to subsequent tables for displacements.

[2], [3], [4] Vertical displacements for modulus of elasticity values of 35,000 MPa, 40,000 MPa, and 43,700 MPa respectively.

[5], [6], [7] Transverse displacements for modulus of elasticity values of 35,000 MPa, 40,000 MPa, and 43,700 MPa respectively.

In a summary, the results presented in this section, as well as results from additional time-history analyses with different excitations, all indicated that in overall, the modulus of elasticity of E_c=40,000 MPa provides average response values compared with those obtained for E_c=35,000 MPa and 43,700 MPa. The average variations of the responses for values of the modulus of elasticity ranging between E_c=35,000 MPa and E_c=43,700 MPa are less than 8.5% relative to the responses for E_c=40,000 MPa. Given these findings, one can easily estimate the maximum responses for different values of the modulus of elasticity based on computed response values for E_c=40,000 MPa. Based on these considerations, the modulus of elasticity of E_c=40,000 MPa was used in the analyses in this study.

5.6 Results from Response-Spectrum Analysis

Response-spectrum analyses were conducted using the design and the evaluation models. The objective of these analyses was to compare the design responses with those resulting from the seismic hazard parameters for the bridge location provided recently by the Geological Survey of Canada (GSC).

In the analysis of the design model, the horizontal and vertical seismic actions were represented by the horizontal and vertical design spectra respectively. The horizontal design spectrum was given in the design criteria (JMS 1996), and the vertical spectrum was taken as 2/3 of the horizontal spectrum, as specified in these criteria. For the evaluation model, the horizontal seismic actions were represented by the uniform hazard spectrum (UHS) computed by Geological Survey of Canada. The vertical actions were represented by a spectrum that was taken as 2/3 of the UHS, which is a commonly accepted approach for defining vertical design spectra relative to horizontal spectra (Newmark et al. 1973). The horizontal design spectrum (JMS 1996) and the horizontal uniform hazard spectrum used in the response-spectrum analysis are shown in Fig. 3.1 (Chapter 3).

The results from the response-spectrum analyses are presented in Figures 5.3 and 5.4, and in Table 5.3. Figure 5.3(a) shows the envelopes of the positive longitudinal moments in the

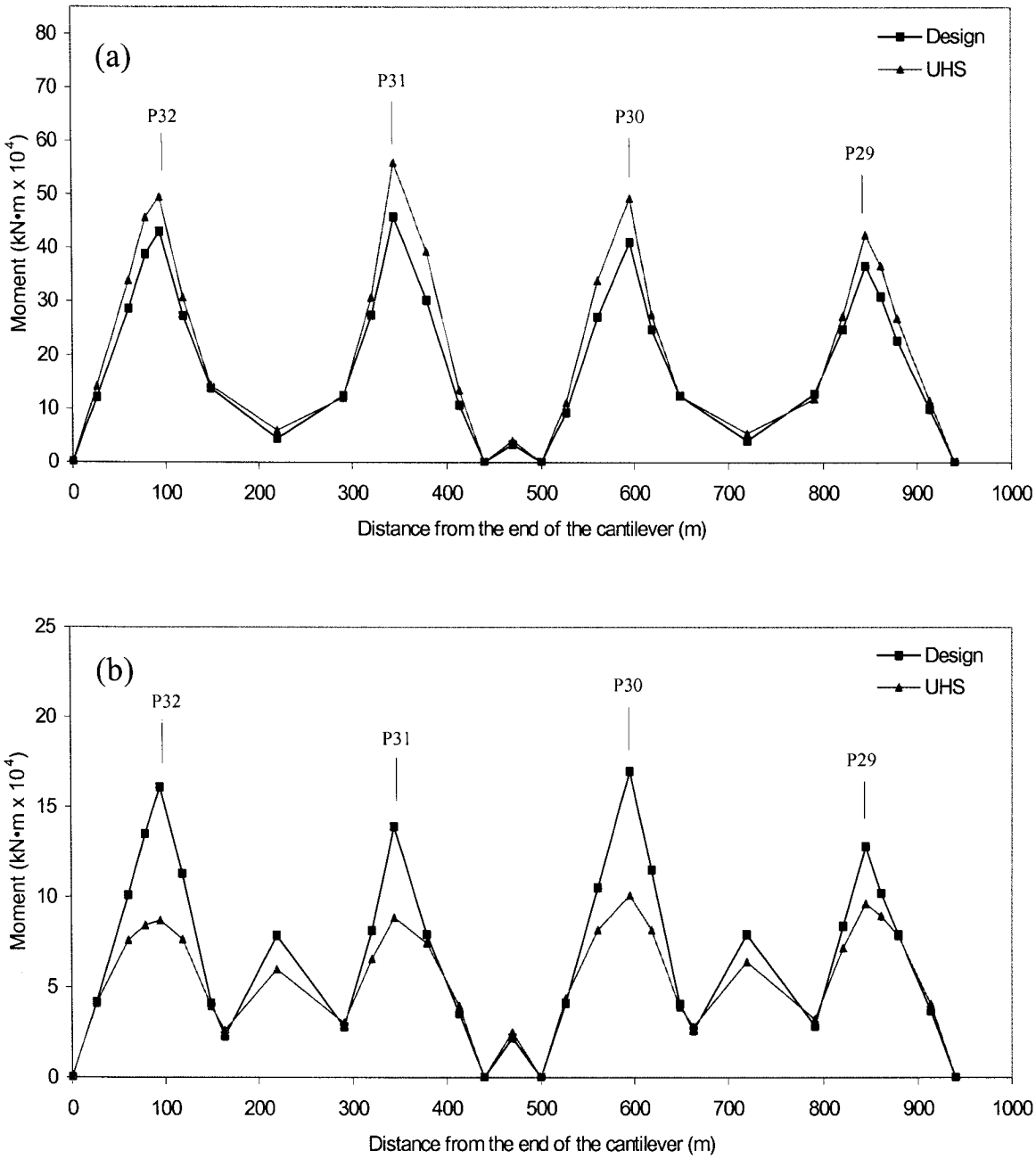

Figure 5.3 Envelopes of positive moments in the bridge girder for seismic actions represented by the design and the uniform hazard spectra, (a) Longitudinal moments, (b) Transverse moments.

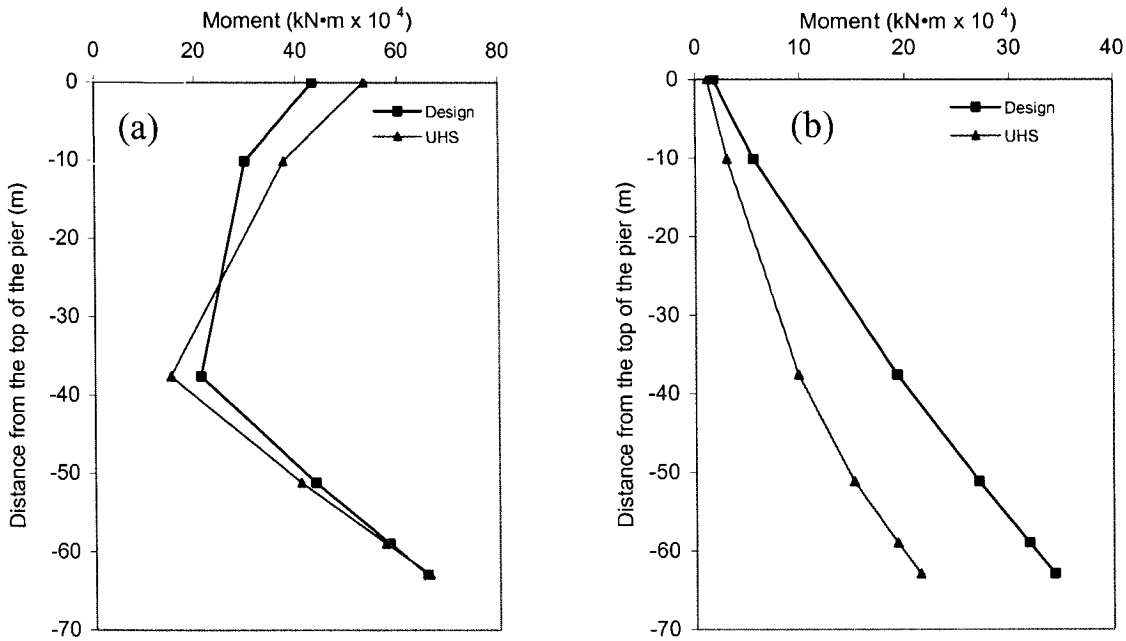

Figure 5.4 Envelopes of positive moments in pier P31 for seismic actions represented by the design and the uniform hazard spectra, (a) In longitudinal direction, (b) In transverse direction.

Table 5.3 Maximum vertical and transverse displacements of the bridge girder for seismic actions represented by the design and uniform hazard spectra.

Location	Vertical displacement (mm)		Transverse displacement (mm)	
	Design	Evaluation	Design	Evaluation
End of cantilv., left of P32	171	123	129	50
Pier P32	0	0	43	28
Mid-span (P31-P32)	93	108	153	59
Pier P31	0	0	50	27
Bearing (left)	156	156	107	46
Middle of drop-in girder	78	74	105	43
Bearing (right)	163	148	164	62
Pier P30	0	0	59	31
Mid-span (P29-P30)	86	101	167	65
Pier P29	0	0	62	30
End of cantilv., right of P29	153	111	103	45

bridge girder for seismic actions in the longitudinal direction, and Fig. 5.3(b) shows the envelopes of the positive transverse moments for seismic actions in the transverse direction. The envelopes designated "design" in the figures are those resulting from the analysis of the design model with seismic actions represented by the horizontal and vertical design spectra, and the envelopes designated "UHS" are those obtained from the analysis of the evaluation model with seismic actions represented by the GSC horizontal and vertical uniform hazard spectra. Figure 5.3(a) shows that for the excitations in the longitudinal direction, the evaluation envelope is somewhat higher than the design envelope. This is because the periods of the predominant longitudinal and vertical modes are shorter than approximately 1.5 s, i.e. these are within the range in which the uniform hazard spectrum is higher than the design spectrum (see Fig. 3.1, Chapter 3).

The positive moment envelopes for pier P31 for excitations in the longitudinal and transverse directions are shown in Figures 5.4(a) and 5.4(b) respectively. As for the girder, the values of the evaluation envelope resulting from the excitation in the longitudinal direction (Fig. 5.4(a)) are somewhat larger than those of the design envelope in the upper 25 m of the pier. For the excitation in the transverse direction (Fig. 5.4(b)), the evaluation envelope has smaller values than the design envelope. The reasons for this are explained above, in the discussion for the girder.

Table 5.3 shows the maximum values of the vertical and transverse displacements at selected sections of the bridge girder for excitations in the longitudinal and transverse directions. The meanings of the designations "design" and "UHS" are the same as those for the bending moments. It can be seen from the table that with the exception of the vertical displacements of the evaluation model in mid-spans of the rigid frames (P29-P30 and P31-P32) which are somewhat larger than the design values, in all other cases the design values are larger than the evaluation values.

It is useful to mention that the *design envelopes* of the bending moments (Figs. 5.3 and 5.4) and the *design* values for the vertical and transverse displacements (Table 5.3) are

considerd as reference response parameters for the seismic evaluation of the bridge, and these are used in all subsequent comparisons in this Chapter.

5.7 Results from Time-History Analysis

5.7.1 Overview

Given the uncertainties in the estimation of the seismic hazard for eastern Canada discussed in Chapter 3 (Section 3.2), a number of time-history analyses were conducted using excitation motions well beyond the scenario earthquake motions for the bridge location determined from the seismic hazard analysis (see Section 3.3). In total, five groups of different seismic excitations were considered.

Because of lack of strong seismic motion records in eastern Canada, two ensembles of ground motion records obtained during strong earthquakes around the world were used in this study. The ensembles are described in Naumoski et al. (1988, 1993) and are characterized by different peak ground acceleration to peak ground velocity ratios (A/V ratios). The average A/V ratio (A in g, and V in m/s) of the records of one of the ensembles is 2.06, and that of the other ensemble is 0.48. Based on the A/V ratios of the records, the ensembles are referred to as the high and low A/V ensembles. In general, high A/V ratios are characteristics of seismic motions from small to moderate earthquakes at short distances, and low A/V ratios are characteristics of seismic motions from large earthquakes at large distances. Regarding the frequency content, high A/V motions normally have a high frequency content, and low A/V motions have a low frequency content. Seismic motions with a high frequency content are characterized by predominant frequencies higher than approximately 2 Hz (i.e. periods lower than 0.5 s), and seismic motions with a low frequency content are characterized by predominant frequencies lower than 2 Hz (i.e. periods longer than 0.5 s).

In addition to the foregoing ensembles, ground motion records obtained during the 1988 Saguenay, Quebec earthquake, and the 1982 Miramichi, New Brunswick earthquake were used as excitation motions. Also, stochastic seismic motions generated for eastern Canada were

used. The characteristics of each of the five ensembles are described in more detail in the subsequent sections, in the discussion of the excitation motions used in the analyses. It is believed that the seismic excitations considered in this study cover not only the scenario seismic motions estimated from the seismic hazard analysis but also all possible scenarios of seismic motions that might occur at the bridge location.

5.7.2 High A/V Excitations

It is well known that seismic ground motions in eastern Canada are characterized by high frequency content and high A/V ratios (Adams and Halchuk 2003; Naumoski et al. 1988). As discussed above, an ensemble of records with high A/V ratios from strong earthquakes around the world (Naumoski et al. 1988) was adopted for the analysis. The ensemble consisted of 13 pairs of horizontal and vertical records. The characteristics of the earthquakes and the horizontal records are shown in Table 5.4. It can be seen from this table that the magnitudes of the earthquakes are between 5.25 to 6.9. The records were taken at distances ranging from 4 km to 26 km, and have A/V ratios (A in g, and V in m/s) between 1.67 and 2.63, with an average A/V of 2.06. The magnitudes of these earthquakes cover the magnitude range of 6.0 to 6.75 of the scenario earthquakes for the short period ground motion hazard for the bridge location (see Chapter 3).

The excitation motions for the time-history analysis were obtained by scaling the records to a peak ground velocity of 7.1 cm/s, as described in Section 5.2.2. These excitations are referred to as high A/V excitations. Figure 5.5 shows the acceleration response spectra of the scaled horizontal records of the ensemble. For comparison, the design spectrum is superimposed on the figure. It can be seen that the spectra of the records exceed significantly the design spectrum for periods shorter than approximately 0.5 s, and the spectra are well below the design spectrum for periods longer than 0.5 s.

The positive envelopes for bending moments and displacements were computed for each pair of horizontal and vertical motions, applied in each of the longitudinal and transverse directions of the evaluation model. For each direction, the envelope values resulting from the

13 excitations were statistically analyzed to compute the mean (M) and the mean plus one standard deviation (M+1SD) values.

Table 5.4 Characteristics of high A/V excitations.

Rec No.	Earthquake	Date	Magn	Recording site	Epic. dist. (km)	Comp.	A (g)	V (m/s)	A/V	Soil type
1	Parkfield California	June 27 1966	5.6	Temblor No. 2	7	N65W	0.269	0.145	1.86	Rock
2	Parkfield California	June 27 1996	5.6	Cholame, Shandon No. 5	5	N85E	0.434	0.255	1.70	Rock
3	San Francisco California	Mar. 22 1957	5.25	Golden Gate Park	11	S80E	0.105	0.046	2.28	Rock
4	San Francisco California	Mar. 22 1957	5.25	State Bldg., S.F.	17	S09E	0.085	0.051	1.67	Stiff soil
5	Helena Montana	Oct. 31 1935	6.0	Caroll College	8	N00E	0.146	0.072	2.03	Rock
6	Lytle Creek	Sep. 12 1970	5.4	Wrightwood, California	15	S25W	0.198	0.096	2.06	Rock
7	Oroville California	Aug. 1 1975	5.7	Seism. Station Oroville	13	N53W	0.084	0.044	1.91	Rock
8	San Fernando California	Feb. 9 1971	6.4	Pacoima Dam	4	S74W	1.075	0.577	1.86	Rock
9	San Fernando California	Feb. 9 1971	6.4	Lake Hughes Station 4	26	S21W	0.146	0.085	1.72	Rock
10	Nahanni, NWT, Canada	Dec. 23 1985	6.9	Site 1, Iverson	7.5	LONG.	1.101	0.462	2.38	Rock
11	Honshu Japan	Apr. 5 1966	5.4	Hoshina-A	4	N00E	0.270	0.111	2.43	Stiff soil
12	Monte Negro Yugoslavia	Apr. 9 1979	5.4	Albatros Hotel Ulcinj	12.5	N00E	0.042	0.016	2.63	Rock
13	Banja Luka Yugoslavia	Aug. 13 1981	6.1	Seism. Station Banja Luka	8.5	N90W	0.074	0.032	2.31	Rock

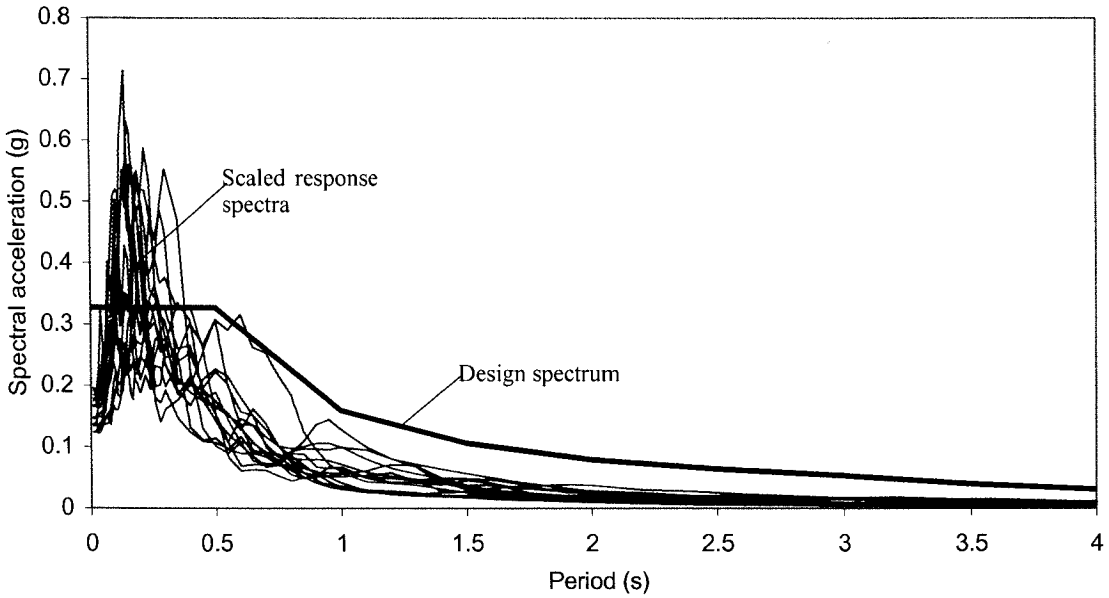

Figure 5.5 Design spectrum and scaled response spectra of high A/V excitations; 5% damping.

The M+1SD envelopes of the positive longitudinal moments in the bridge girder for excitation motions in the longitudinal direction are shown in Fig. 5.6(a), and those of the positive transverse moments for excitation motions in the transverse direction are shown in Fig. 5.6(b). These envelopes are designated "High A/V" referring to the high A/V seismic excitations used in the analysis. Similarly, Figs. 5.7(a) and 5.7(b) show the M+1SD envelopes of the moments in pier P31 for excitation motions in the longitudinal and transverse directions respectively. The M+1SD values for vertical and transverse displacements of the bridge girder are given in Table 5.5. A general observation from the figures and the table is that the values of the high A/V envelopes for both the moments and displacements are much smaller than those of the design envelopes. This was not surprising since the periods of the predominant modes are all within the intermediate and long period ranges (i.e. above approximately 0.5 s) in which the spectra of the excitations are much lower than the design spectrum (Fig. 5.5), and the contributions of the modes with periods below 0.5 s are very small.

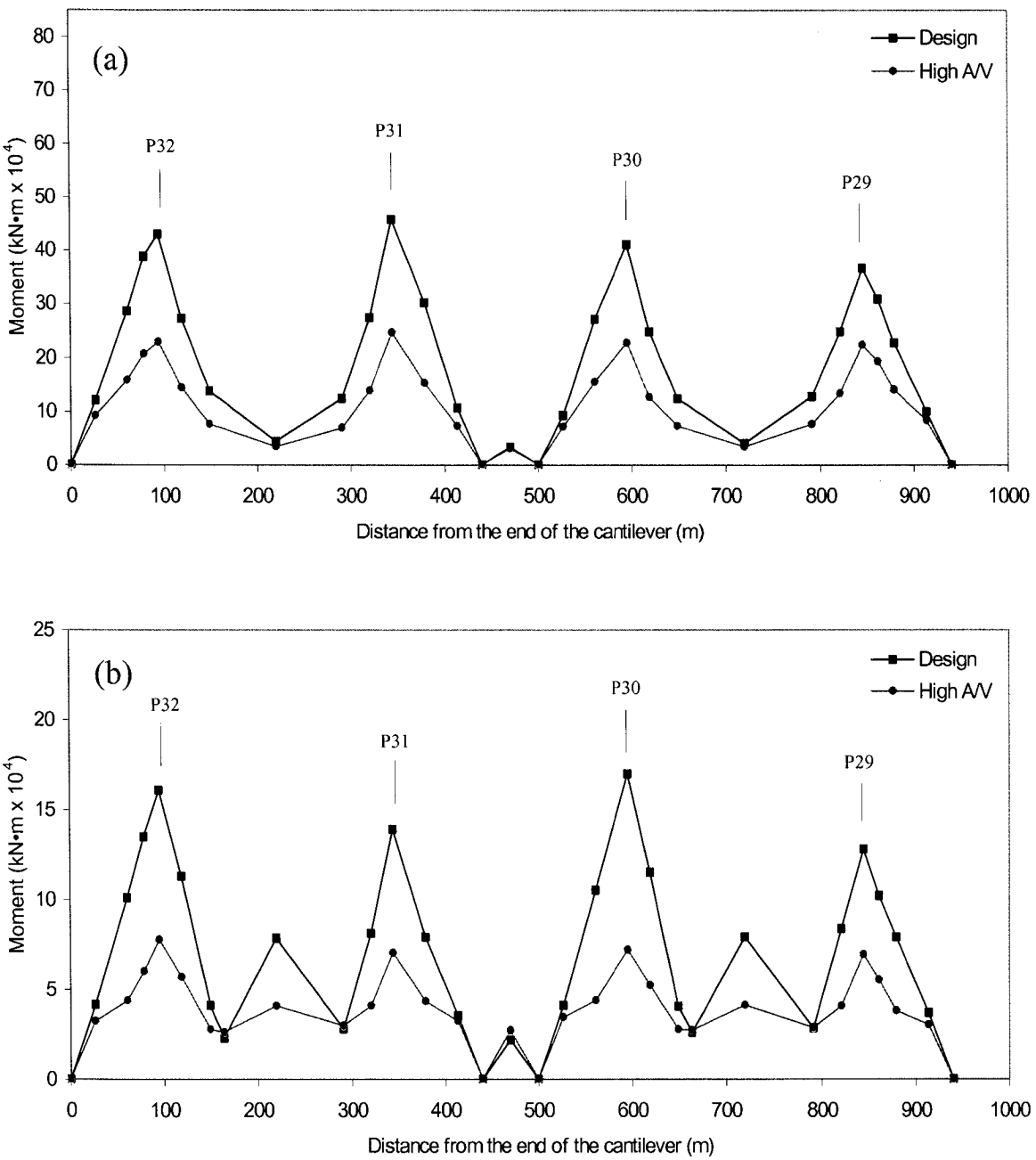

Figure 5.6 Envelopes of positive moments in the bridge girder for design and high A/V excitations: (a) Longitudinal moments, (b) Transverse moments.

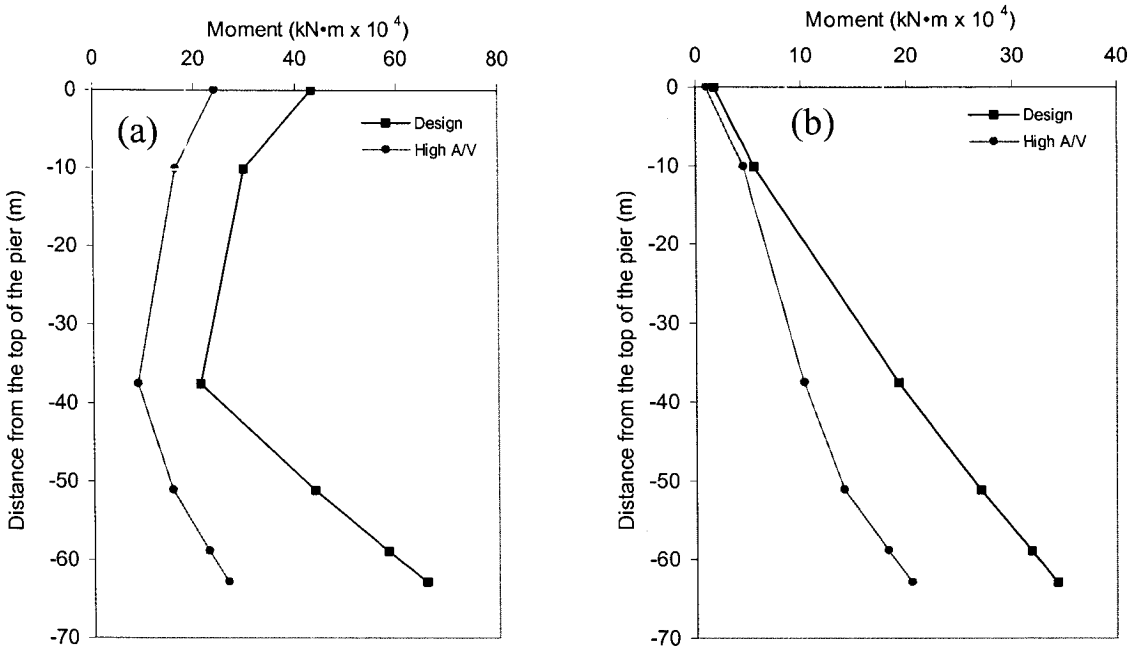

Figure 5.7 Envelopes of positive moments in pier P31 for design and high A/V excitations, (a) In longitudinal direction, (b) In transverse direction.

Table 5.5 Maximum vertical and transverse displacements of the bridge girder for design and high A/V excitations.

Location	Vertical displacement (mm)		Transverse displacement (mm)	
	Design	High A/V	Design	High A/V
End of cantilv., left of P32	171	65	129	41
Pier P32	0	0	43	18
Mid-span (P31-P32)	93	39	153	54
Pier P31	0	0	50	20
Bearing (left)	156	65	107	25
Middle of drop-in girder	78	32	105	37
Bearing (right)	163	73	164	46
Pier P30	0	0	59	18
Mid-span (P29-P30)	86	36	167	56
Pier P29	0	0	62	22
End of cantilv., right of P29	153	62	103	37

5.7.3 Low A/V Excitations

The low A/V ensemble consisted of 15 pairs of horizontal and vertical records of seismic ground motions (Naumoski et al. 1993). The characteristics of the horizontal records of the ensemble are given in Table 5.6. The A/V ratios of the records are between 0.37 and 0.58. The records were taken during strong earthquakes with magnitudes ranging from 6.3 to 8.1. The distances at which the records were taken were within the range from 38 km to 469 km. Both the magnitudes and the distances cover the magnitude and distance ranges of the scenario earthquakes for short and long period ground motion hazards for the bridge location determined from the seismic hazard analysis (see Chapter 3). As shown in the table, there are 8 records obtained at distances of 38 km to 97 km from three earthquakes with magnitudes of 6.3, 6.4, and 7, that can be considered representative of the scenario earthquake for short period ground motion hazard, and there are 4 records at distances of 373 km to 469 km from earthquakes with magnitudes of 7.8 and 8.1 that represent the long period ground motion hazard.

Figure 5.8 shows the acceleration response spectra of the horizontal records of the low A/V ensemble scaled to the peak ground velocity of 7.1 cm/s corresponding to the annual probability of exceedance of 0.00027. The design spectrum is also included in the figure. It can be seen that the spectra for the low A/V records are all enveloped by the design spectrum. Given this, no time-history analyses were conducted for this ensemble.

Table 5.6 Characteristics of low A/V excitations.

Rec No.	Earthquake	Date	Magn	Recording site	Epic. dist. (km)	Comp.	A (g)	V (m/s)	A/V	Soil type
1	Long Beach California	Mar. 10 1933	6.3	Subway Terminal, L.A.	59	N51W	0.097	0.237	0.41	Rock
2	Long Beach California	Mar. 10 1933	6.3	Subway Terminal, L.A.	59	N39E	0.064	0.173	0.37	Rock
3	San Fernando California	Feb. 9 1971	6.4	4680 Wilshire Blvd., L.A.	38	N15E	0.117	0.215	0.54	Stiff soil
4	San Fernando California	Feb. 9 1971	6.4	4680 Wilshire Blvd., L.A.	38	N75W	0.084	0.209	0.40	Stiff soil
5	San Fernando California	Feb. 9 1971	6.4	2500 Wilshire Blvd., L.A.	40	N61W	0.101	0.193	0.52	Stiff soil
6	Loma Prieta California	Oct. 17 1989	7.0	Yerba Buena Island	95	N90	0.067	0.147	0.46	Rock
7	Loma Prieta California	Oct. 17 1989	7.0	Pacific Hights, S.F.	97	N360	0.047	0.099	0.59	Rock
8	Loma Prieta California	Oct. 17 1989	7.0	Pacific Hights, S.F.	97	N270	0.061	0.143	0.43	Rock
9	Alaskan Subd. Zone	Oct. 9 1985	6.5	Ivanof, Alaska	129	N247	0.009	0.18	0.50	Rock
10	Mexico Earthquake	Sep. 19 1985	8.1	U.N.A.M., Mexico City	379	N90W	0.034	0.094	0.36	Rock
11	Mexico Earthquake	Sep. 19 1985	8.1	M. Vibradora C.U., M. City	379	S00E	0.038	0.092	0.41	Rock
12	Mexico Earthquake	Sep. 19 1985	8.1	Sismic Puebla, Mexico City	469	N90E	0.033	0.066	0.50	Stiff soil
13	Tangshan Earthq., China	July 28 1976	7.8	Hongshan, Hebei	373	S00E	0.007	0.14	0.50	Rock
14	Tangshan Earthq., China	July 28 1976	7.1	Beijing Dipl. Appartment	170	S00E	0.024	0.041	0.58	Stiff soil
15	Tangshan Earthq., China	Nov. 15 1976	6.9	Beijing Hotel	122	N90E	0.026	0.045	0.58	Stiff soil

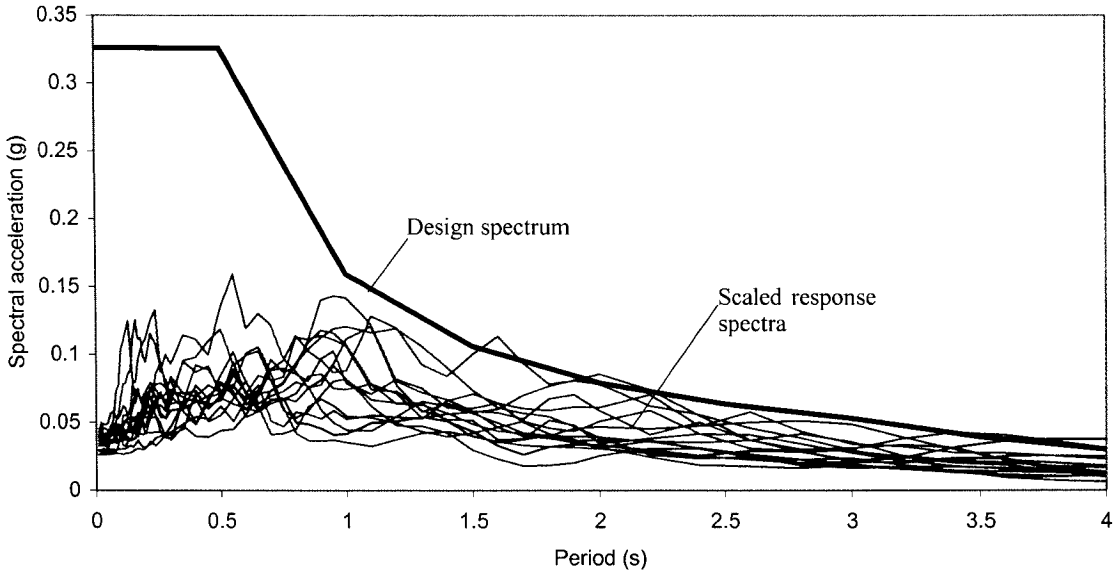

Figure 5.8 Design spectrum and scaled response spectra of low A/V excitations; 5% damping.

5.7.4 Saguenay Earthquake Excitations

It was of special importance for this study to investigate the performance of the bridge when subjected to seismic motions from earthquakes in eastern Canada. On November 25, 1988, an earthquake of magnitude of 5.7 occurred in the Saguenay region of the province of Quebec. This was the most significant earthquake in the past 50 years in eastern North America. Ground motion records were obtained at 16 sites at distances ranging from 43 km to 525 km (Munro and Weichert 1989; Friberg et al. 1988). The response spectra for all horizontal records were scaled to the peak ground velocity for the bridge location of 7.1 cm/s and were compared with the design spectrum. Based on this comparison, 5 horizontal records and the companion vertical records were selected for the analysis. The characteristics of the selected records are shown in Table 5.7. The scaled spectra of the records together with the design spectrum are shown in Fig. 5.9. Records No. 1 to No. 4 were the strongest records, and record No. 5 was selected since it is the only one that has somewhat lower frequency content than the other records. As shown in Table 5.7, the records are characterized by very high A/V ratios that range from 2.2 to 8.5. These are much larger ratios than those of "typical" high A/V records

discussed in Section 5.7.2. The unusually high A/V ratios indicate to a very high frequency content, which can be clearly seen from the response spectra. The spectra show that the frequencies of the Saguenay earthquake motions are higher than 4 Hz (i.e. the periods are lower than approximately 0.25 s). It can also be seen that the scaled spectra of the Saguenay earthquake motions are significantly higher than the design spectrum for periods below 0.25 s. The highest spectra (for records No. 2 and No. 3) exceed the design spectrum by a factor of approximately 5.

Table 5.7 Characteristics of Saguenay earthquake excitations.

Rec. No.	Recording site	Epic. dist. (km)	Compo-nent	A (g)	V(m/s)	A/V
1	St-Ferreol, Quebec	114	N270	0.0970	0.0245	3.96
2	Chocoutimi-Nord, Quebec	43	N214	0.1070	0.0151	7.09
3	St-Andre, Quebec	64	N00	0.1560	0.0183	8.52
4	Dickey, Maine	199	N90	0.0916	0.0300	3.05
5	Newcomb, N.Y.	525	N15	0.0022	0.0010	2.20

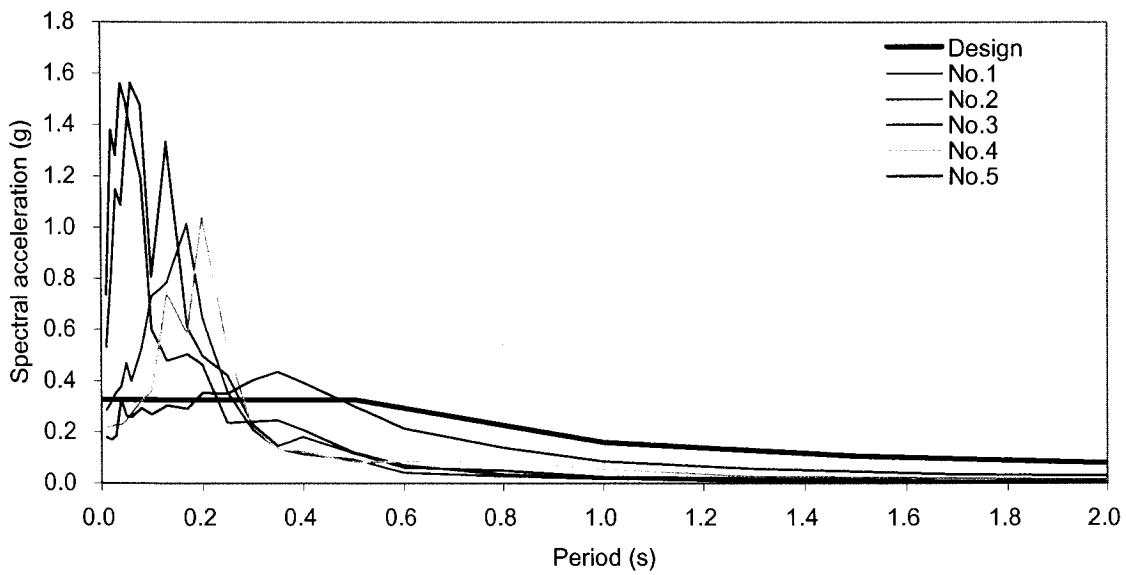

Figure 5.9 Design spectrum and scaled response spectra of Saguenay earthquake excitations; 5% damping.

The results from the time-history analyses for the selected seismic excitations are shown in Figs. 5.10 and 5.11, and in Tables 5.8 and 5.9. Figures 5.10 and 5.11 show the moment envelopes for the bridge girder and pier P31 respectively. The designation of the envelopes (No. 1 to No. 5) in the figures corresponds to the designation of the records in Table 5.7. The longitudinal and transverse moment envelopes for the bridge girder (Figs. 10(a) and 10(b)) are lower than the design envelope at most sections. An exception from this is the section at the middle of the drop-in girder where the transverse moments for most excitations are larger than the design values (Fig. 5.10(b)). This is because the period of the dominant transverse mode of the drop-in girder coincides with the dominant periods of the excitations.

Figure 5.11(a) and 5.11(b) show that the values of the moment envelopes for pier P31 resulting from time-history analyses are all smaller than the design values. This was expected since for all excitations, the moments at the girder section at pier P31 are significantly smaller than the design moment (see Figs. 5.10(a) and 5.10(b)).

The vertical and transverse displacements of the bridge girder are shown in Tables 5.8 and 5.9 respectively. It can be seen that all displacements are smaller than the design values.

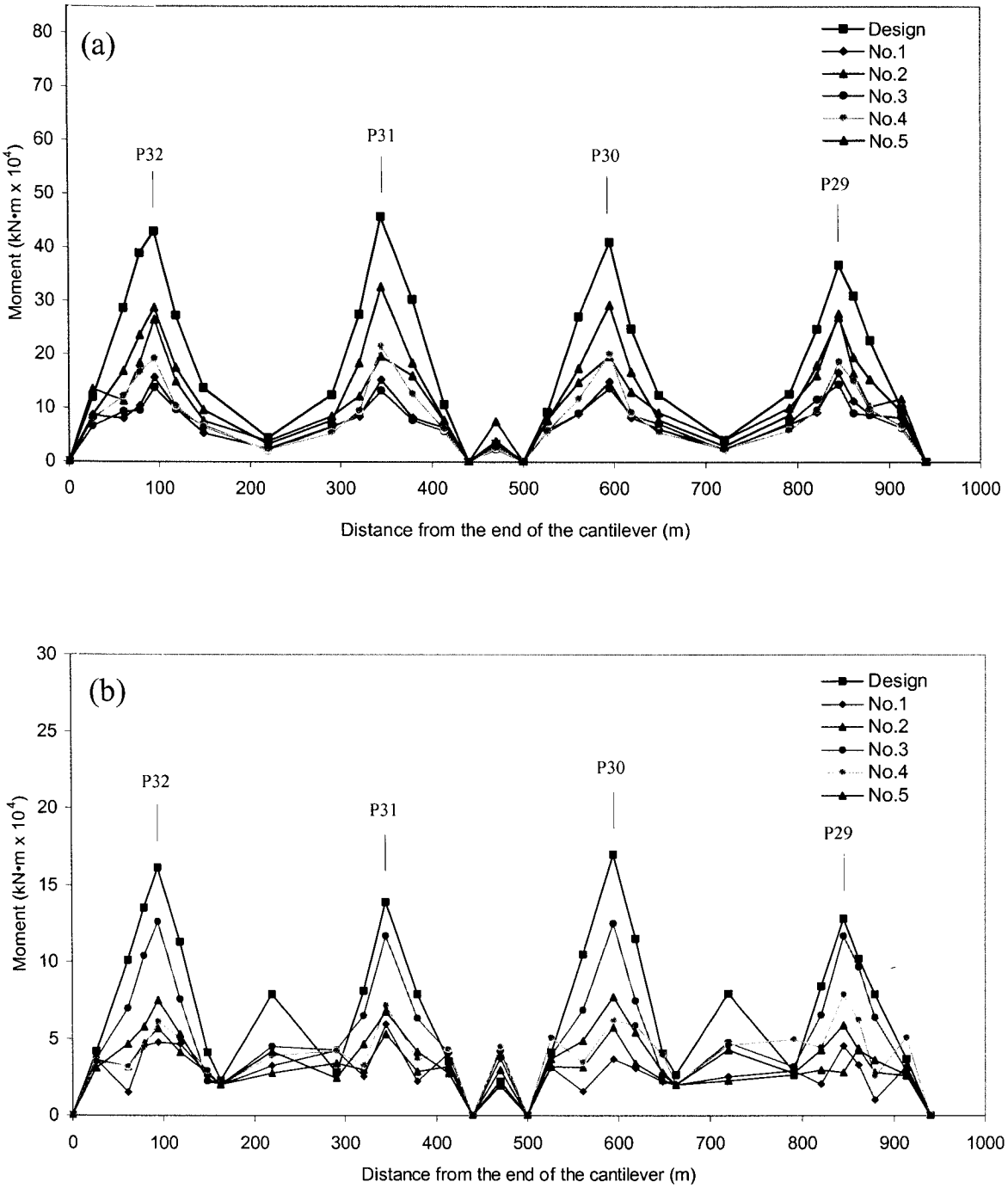

Figure 5.10 Envelopes of positive moments in the bridge girder for design and Saguenay earthquake excitations: (a) Longitudinal moments, (b) Transverse moments.

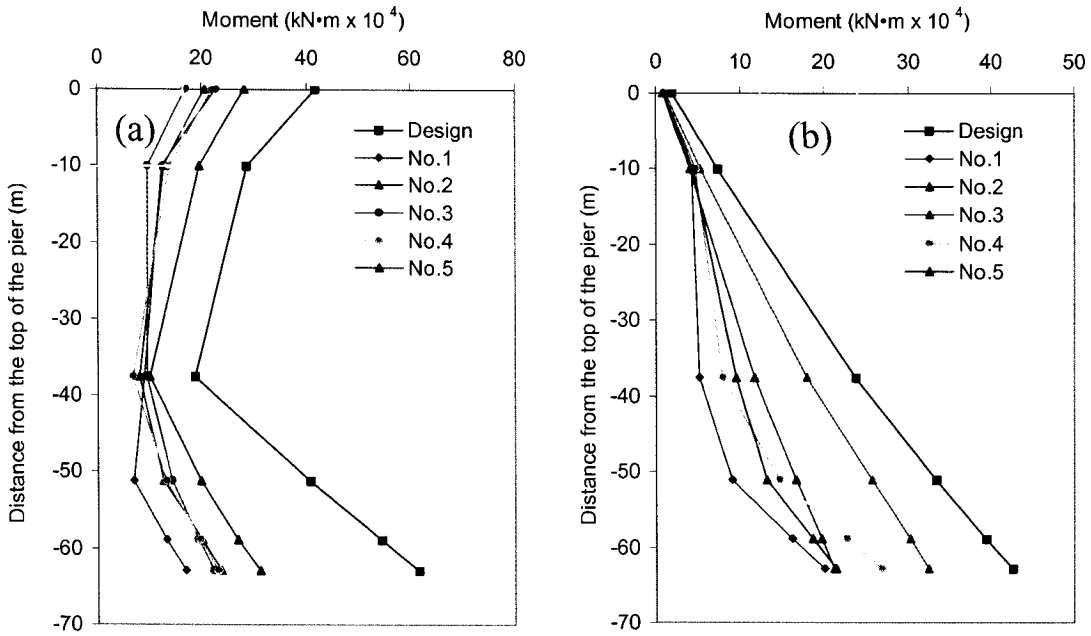

Figure 5.11 Envelopes of positive moments in pier P31 for design and Saguenay Earthquake excitations, (a) In longitudinal direction, (b) In transverse direction.

Table 5.8 Maximum vertical displacements of the bridge girder for design and Saguenay earthquake excitations.

Location	Vertical displacement (mm)					
	Design	No. 1	No. 2	No. 3	No. 4	No. 5
End of cantilv., left of P32	171	20	51	63	40	68
Pier P32	0	0	0	0	0	0
Mid-span (P31-P32)	93	16	20	14	26	40
Pier P31	0	0	0	0	0	0
Bearing (left)	156	20	51	50	46	79
Middle of drop-in girder	78	15	27	17	19	38
Bearing (right)	163	21	56	67	50	88
Pier P30	0	0	0	0	0	0
Mid-span (P29-P30)	86	17	19	13	24	39
Pier P29	0	0	0	0	0	0
End of cantilv., right of P29	153	20	49	62	34	63

Table 5.9 Maximum transverse displacements of the bridge girder for design and Saguenay earthquake excitations.

Location	Transverse displacement (mm)					
	Design	No. 1	No. 2	No. 3	No. 4	No. 5
End of cantilv., left of P32	129	7	51	80	18	48
Pier P32	43	5	18	27	12	18
Mid-span (P31-P32)	153	10	48	74	21	59
Pier P31	50	6	26	39	13	18
Bearing (left)	107	5	63	98	18	29
Middle of drop-in girder	105	9	62	95	21	33
Bearing (right)	164	5	61	94	16	49
Pier P30	59	5	25	39	16	22
Mid-span (P29-P30)	167	8	55	85	23	55
Pier P29	62	6	32	49	15	24
End of cantilv., right of P29	103	6	70	108	18	31

In summary, the results show that the bridge would perform quite well when subjected to Saguenay earthquake excitations with intensities corresponding to the peak ground velocity of 7.1 cm/s obtained from seismic hazard analysis for the bridge location. This is because the predominant periods of the ground motions are well below the range of the natural periods of the predominant modes of the bridge.

5.7.5 Miramichi Earthquake Excitations

In 1982, several earthquakes occurred in the Miramichi region of the province of New Brunswick (Weichert et al. 1982). The epicentres were approximately 150 km from the bridge site. Ground motion records are available for two of these earthquakes, one of which with a magnitude of 5 occurred on March 31, 1982 and the other one occurred on May 6, 1982. Records from the first event were obtained at 4 sites, and from the second event at one site. All the records were obtained very close to the epicentres of the earthquakes. These are the closest records to the bridge ever recorded. By considering the response spectra, three records representing the strongest motions during the earthquakes were selected for this study. The characteristics of the selected horizontal records are shown in Table 5.10, and their response

spectra scaled to peak ground velocity of 7.1 cm/s are shown in Fig. 5.12. It can be seen from the table that the records are characterized by extremely high A/V ratios. The values of the A/V ratios of the records of the March 31 event are both approximately 11, and these are much higher than those of "typical" high A/V records (Section 5.7.2) and the Saguenay earthquake records (Section 5.7.4). Consequently, the ground motions from the Miramichi earthquakes are dominated by very short period (i.e. very high frequency) motions. This can be seen from the response spectra, which show that the predominant periods of the selected records are approximately 0.04 s (i.e. frequency of 25 Hz). Figure 5.12 also shows that for the period of 0.04 s, the spectral acceleration for the strongest motion (Rec. No. 1) is approximately 9 times larger than the value of the design spectrum.

Table 5.10 Characteristics of Miramichi earthquake excitations.

Rec. No.	Date of earthquake	Recording site	Compo-nent	A (g)	V (m/s)	A/V
1	March 31, 1982	Holmes Lake	N18	0.143	0.0131	10.92
2	March 31, 1982	Mitchell Lake Road	N28	0.202	0.0181	11.16
3	May 6, 1982	Loggie Lodge	N99	0.110	0.0171	6.43

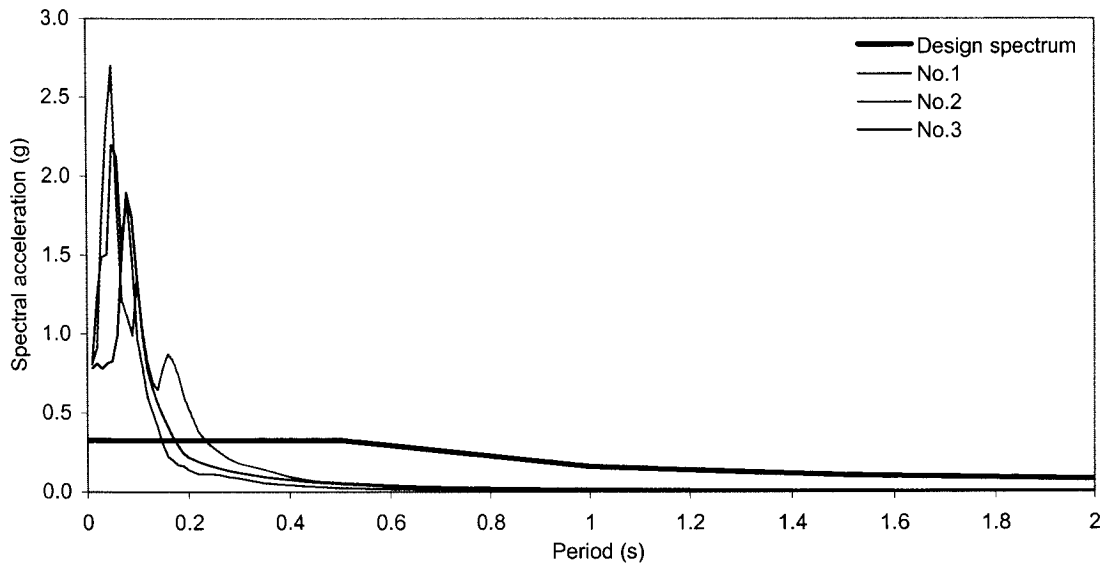

Figure 5.12 Design spectrum and scaled response spectra of Miramichi earthquake excitations; 5% damping.

The moment envelopes obtained from the time-history analysis for each of the selected motions are shown in Figs. 5.13 and 5.14. The computed envelopes are designated No. 1 to No. 3 and correspond to the record No's in Table 5.10. It can be seen from these figures that the values of the moment envelopes for the bridge girder and for pier P31, resulting from the time-history analysis, are all significantly smaller than the values of the design envelope at all sections. The maximum vertical and transverse displacements (Table 5.11) obtained from the time-history analysis are also much smaller than the design values at all sections. As for the Saguenay earthquake excitations, this is because the predominant periods of the ground motions of the Miramichi earthquake excitations are well below the range of the natural periods of the predominant modes of the bridge.

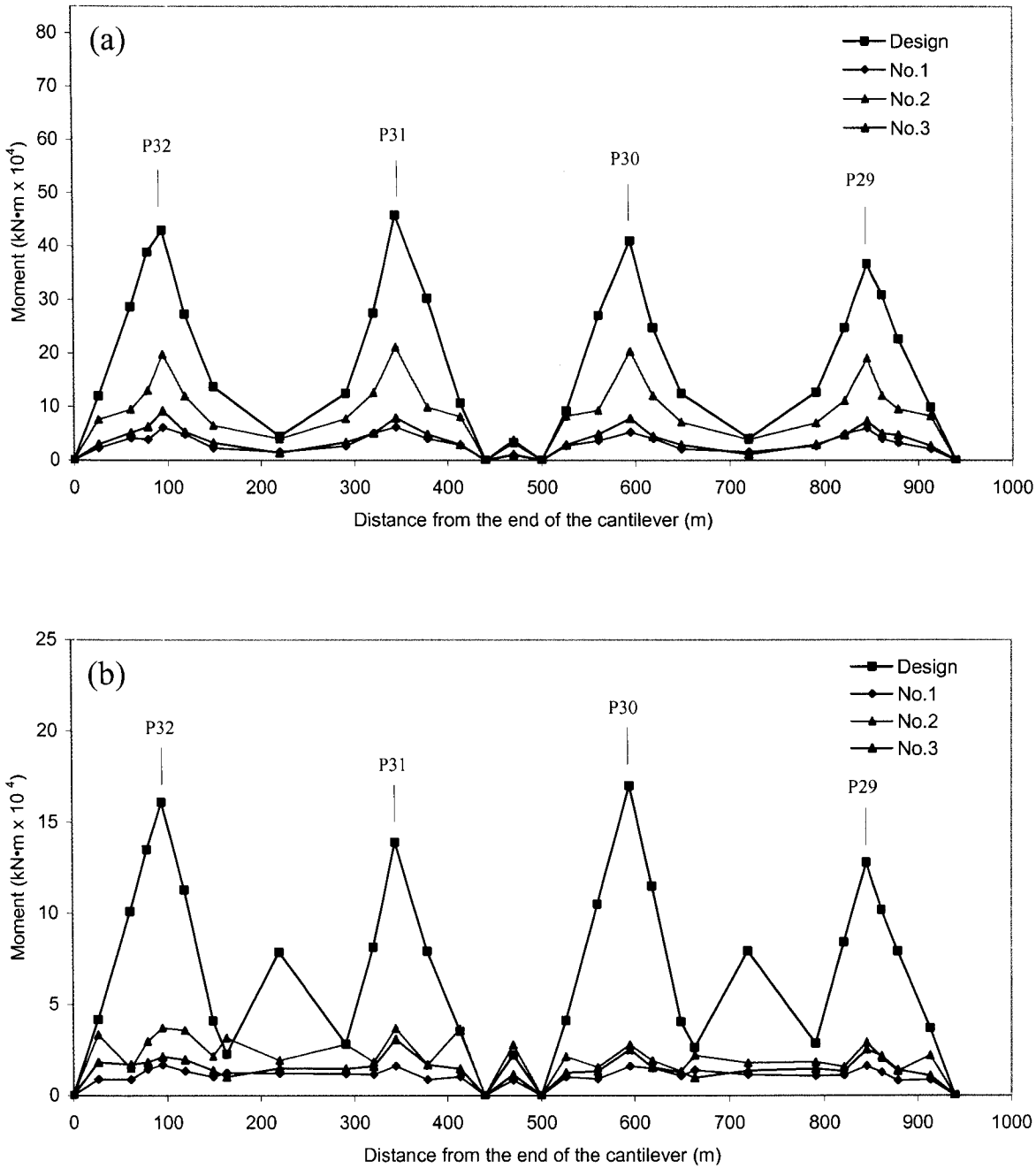

Figure 5.13 Envelopes of positive moments in the bridge girder for design and Miramichi earthquake excitations: (a) Longitudinal moments, (b) Transverse moments.

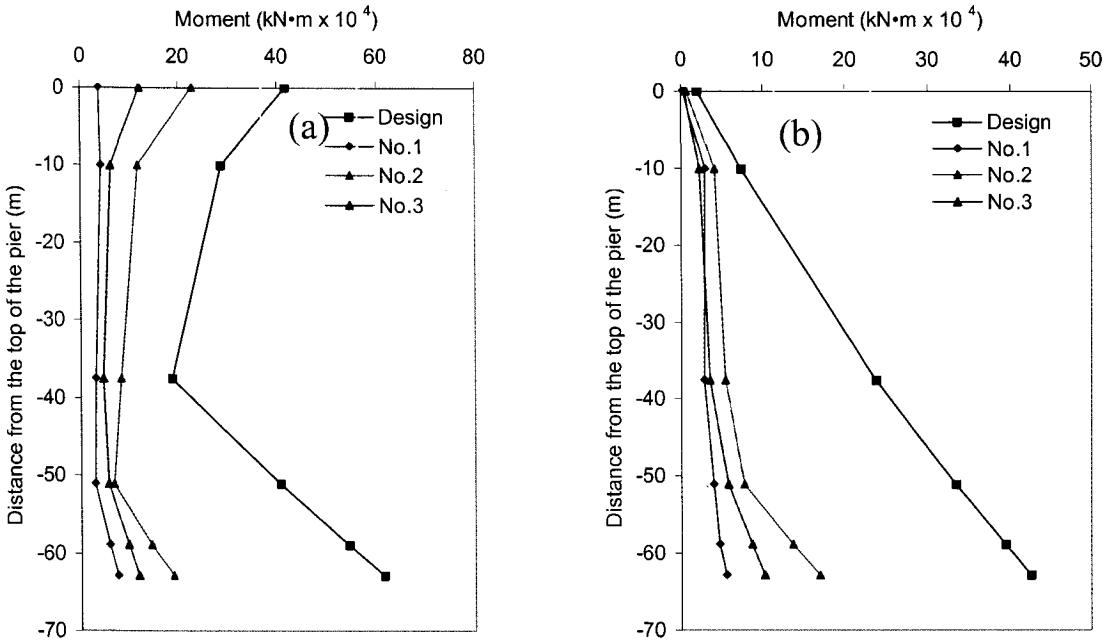

Figure 5.14 Envelopes of positive moments in pier P31 for design and Miramichi earthquake excitations, (a) In longitudinal direction, (b) In transverse direction.

Table 5.11 Maximum vertical and transverse displacements of the bridge girder for design and Miramichi earthquake excitations.

Location	Vertical displacement (mm)				Transverse displacement (mm)			
	Design	No.1	No.2	No.3	Design	No.1	No.2	No.3
End of cantilv., left of P32	171	13	20	13	129	13	24	12
Pier P32	0	0	0	0	43	5	8	4
Mid-span (P31-P32)	93	7	11	6	153	12	22	11
Pier P31	0	0	0	0	50	6	12	6
Bearing (left)	156	16	22	15	107	13	30	18
Middle of drop-in girder	78	9	10	4	105	14	29	15
Bearing (right)	163	13	27	15	164	14	29	14
Pier P30	0	0	0	0	59	6	12	5
Mid-span (P29-P30)	86	7	11	4	167	13	26	12
Pier P29	0	0	0	0	62	7	15	7
End of cantilv., right of P29	153	17	23	11	103	15	33	18

5.7.6 Simulated Excitations

In addition to the "real" records of seismic ground motions discussed above, "simulated" acceleration time histories (i.e. accelerograms) were also used as excitation motions. A method for the generation of such accelerograms is proposed by Atkinson and Beresnev (1998). Using this method, a number of ground motion accelerograms can be simulated for a given location, and specified magnitude and distance. The method is described in detail in Atkinson and Beresnev (1998), and only a summary is presented here. The method begins with the generation of white noise series. The duration of the series is specified as a function of magnitude and distance, based on regional empirical observations. The white noise series are further modified to take into account the characteristics of the earthquake sources, and the attenuation of the motion from the source to the specified location. Finally, the resulting series are multiplied by a factor related to the required probability of exceedance.

According to Tremblay and Atkinson (2001), the uniform hazard spectrum (UHS) for a probability of exceedance of 2% in 50 years (annual probability of 0.000404) can be approximated using a magnitude M=6.0 event to represent the short period hazard, and M=7.0 event to represent the long period hazard. Using the foregoing method, Tremblay and Atkinson (2001) simulated ground motion accelerograms for eastern Canada, for M=6.0 and M=7.0, and for different distances. For each distance, four accelerograms were simulated. Since the duration and the frequency content of simulated accelerograms for a given location depend entirely on the magnitude and the distance, accelerograms generated for a probability of exceedance of 0.000404 and for a given magnitude and distance are also applicable for the probability of exceedance for the bridge of 0.00027 and for the same magnitude and distance, if properly scaled.

To represent the short period hazard motions, the simulated accelerograms for the M=6.0 event were scaled to have the same spectral values at the period of 0.2 s as that of the UHS for the bridge location. Similarly, the long period hazard motions were obtained by scaling the simulated accelerograms for the M=7.0 event to have the same spectral values as

that of the UHS at the period of 2.0 s.

Trial time-history analyses showed that the largest responses are associated with the simulated accelerograms for the largest epicentral distances of each of the events, i.e. R=50 km for the M=6.0 event, and R=100 km for the M= 7.0 event, and therefore, only these accelerograms were considered in this study. The simulated accelerograms for M=6.0, R=50 km are referred to as short period accelerograms, and those for M=7.0, R=100 km are referred to as long period accelerograms. The characteristics of these accelerograms are listed in Table 5.12. The response spectra of the short period accelerograms scaled to the spectral value of the UHS at the period of 0.2 s are shown in Fig. 5.15, and those of the long period accelerograms scaled to the value of the UHS at the period of 2.0 s are shown in Fig. 5.16. The design spectrum is also included in the figures. It can be seen from Fig. 5.15 that the spectra of the short period accelerograms exceed the design spectrum by as much as a factor of 2 for periods below approximately 0.2 s. On the other hand, the spectra of the long period accelerograms (Fig. 5.16) are well below the design spectrum, with the exception of one of the spectra which slightly exceeds the design spectrum at the period of approximately 0.3 s. Given these observations, only the short period accelerograms were used as excitation motions in the time-history analyses.

Table 5.12 Characteristics of simulated excitations.

Magn.-distance combination	Accel. No.	A (g)	V (m/s)	A/V
M=6, R=50 km	1	0.240	0.0718	3.34
	2	0.185	0.0838	2.21
	3	0.202	0.0708	2.85
	4	0.207	0.0683	3.03
M=7, R=100 km	1	0.242	0.150	1.61
	2	0.261	0.207	1.26
	3	0.274	0.153	1.79
	4	0.250	0.161	1.55

The horizontal excitations were represented by the simulated accelerograms. Since no vertical accelerograms were available, vertical excitations were obtained by multiplying the horizontal excitations by a factor of 2/3.

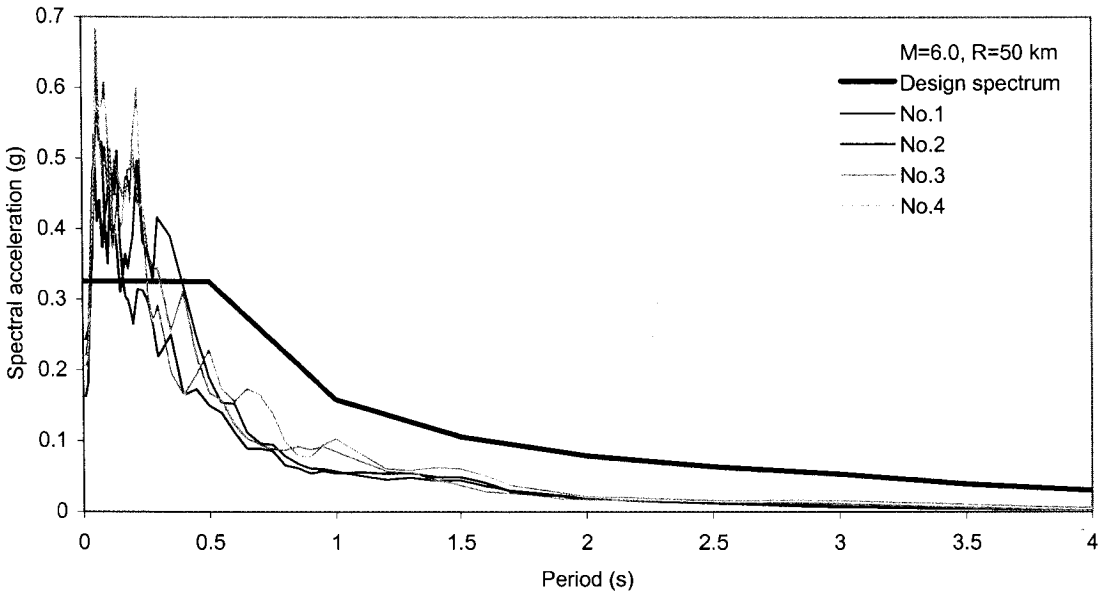

Figure 5.15 Design spectrum and scaled response spectra of simulated short period excitations; 5% damping.

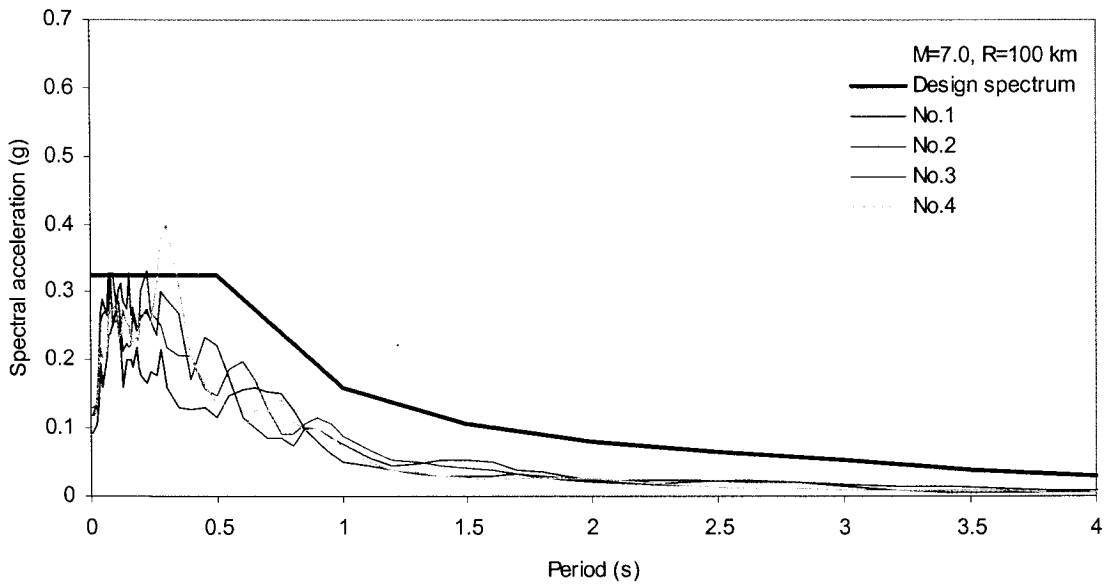

Figure 5.16 Design spectrum and scaled response spectra of simulated long period excitations; 5% damping.

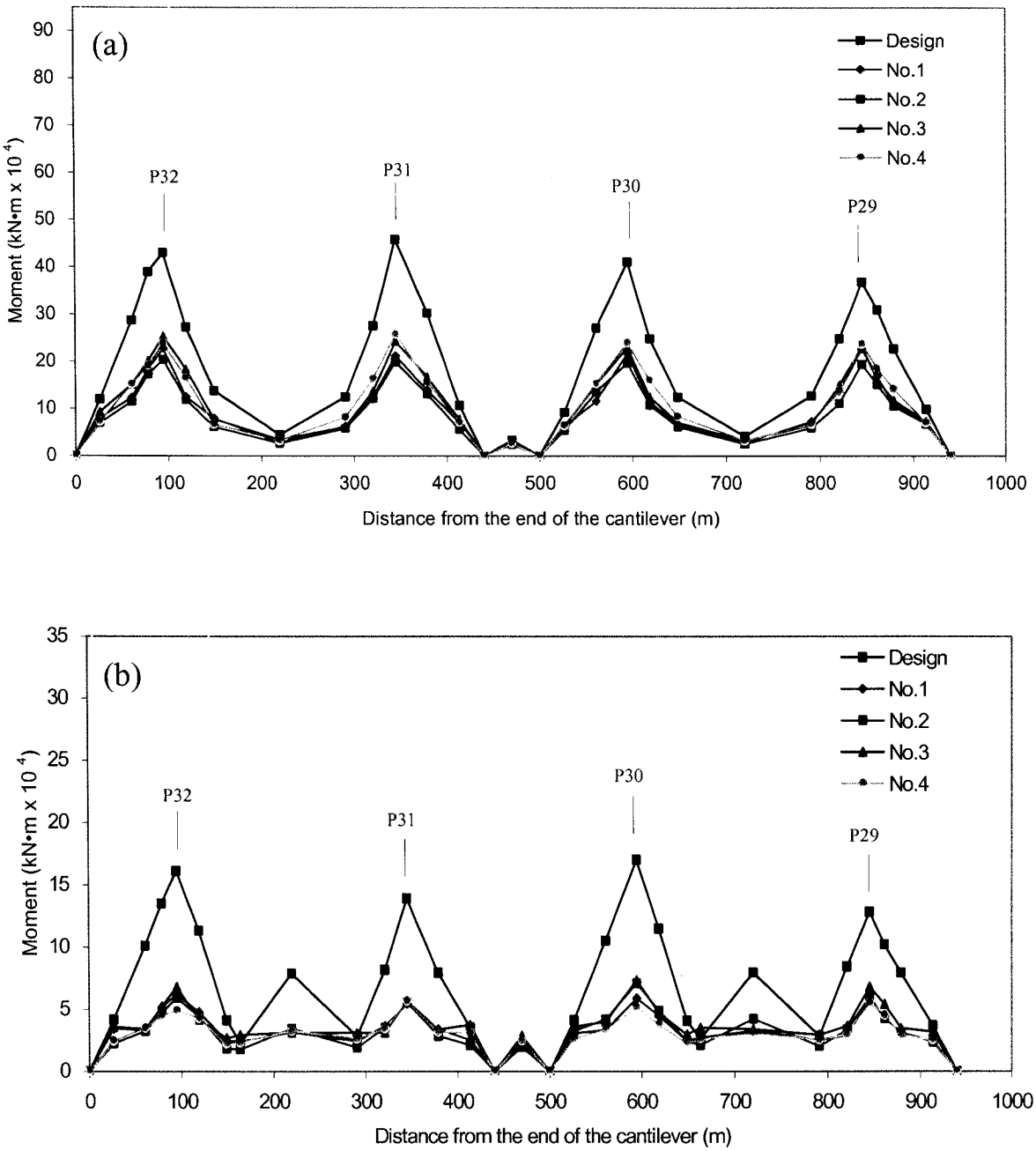

Figure 5.17 Envelopes of positive moments in the bridge girder for design and simulated short period excitations: (a) Longitudinal moments, (b) Transverse moments.

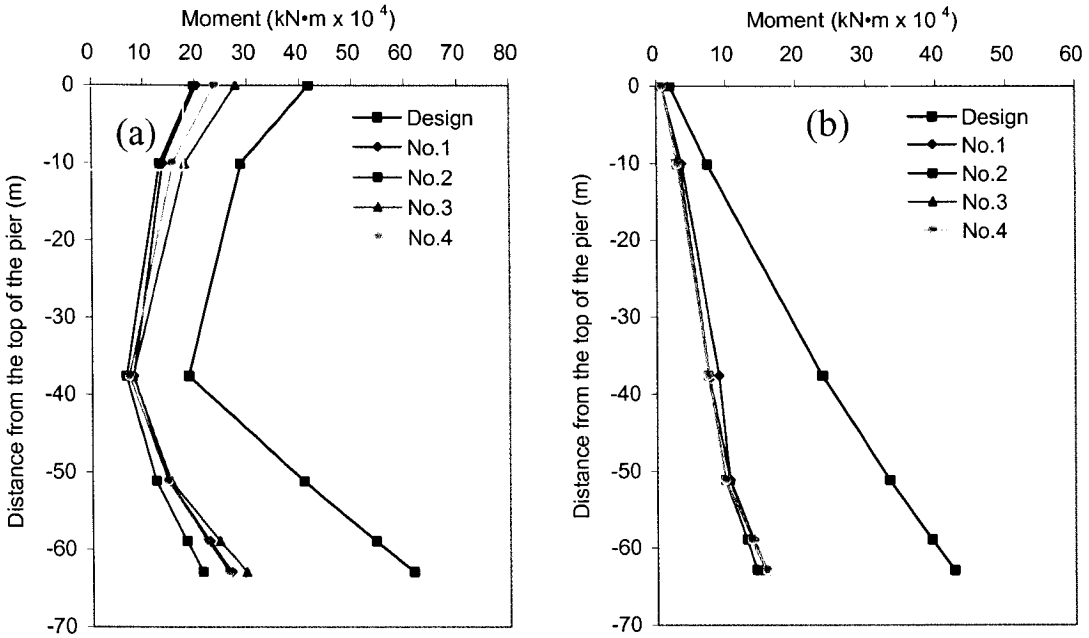

Figure 5.18 Envelopes of positive moments in pier P31 for design and simulated short period excitations, (a) In longitudinal direction, (b) In transverse direction.

The moment envelopes obtained from the analyses are shown in Figs. 5.17 and 5.18. It can be seen from the figures that the moments in both the bridge girder and pier P31 resulting from the simulated excitations are significantly smaller than the design moments. Regarding the displacements, Tables 5.13 and 5.14 show that both the transverse and vertical displacements of the bridge girder are much smaller than the design displacements. Such results were expected considering the similarity of the simulated excitations to the Saguenay and the Miramichi earthquake excitations, and the responses resulting from these two events.

Table 5.13 Maximum vertical displacements of the bridge girder for design and simulated short period excitations.

Location	Vertical displacement (mm)				
	Design	No. 1	No. 2	No. 3	No. 4
End of cantilv., left of P32	171	51	60	51	60
Pier P32	0	0	0	0	0
Mid-span (P31-P32)	93	32	41	39	45
Pier P31	0	0	0	0	0
Bearing (left)	156	58	63	64	64
Middle of drop-in girder	78	28	39	29	32
Bearing (right)	163	61	79	61	67
Pier P30	0	0	0	0	0
Mid-span (P29-P30)	86	32	38	38	47
Pier P29	0	0	0	0	0
End of cantilv., right of P29	153	48	60	49	56

Table 5.14 Maximum transverse displacements of the bridge girder for design and simulated short period excitations.

Location	Transverse displacement (mm)				
	Design	No. 1	No. 2	No. 3	No. 4
End of cantilv., left of P32	129	25	34	28	29
Pier P32	43	14	13	13	11
Mid-span (P31-P32)	153	33	48	35	43
Pier P31	50	17	19	14	13
Bearing (left)	107	23	26	28	30
Middle of drop-in girder	105	25	32	26	34
Bearing (right)	164	24	42	32	36
Pier P30	59	15	15	15	14
Mid-span (P29-P30)	167	31	55	41	43
Pier P29	62	18	17	17	16
End of cantilv., right of P29	103	24	27	30	36

Chapter 6

Discussion and Conclusions

6.1 Discussion

The Confederation Bridge, with its length of 12,910 m, is one of the longest reinforced concrete bridges built over water in the world. It crosses the Northumberland Strait in eastern Canada and connects the province of Prince Edward Island and the province of New Brunswick. The bridge was designed for a service life of 100 years, which is twice the service life of typical highway bridges.

The main objective of this study was to evaluate the performance of the bridge when subjected to seismic excitations representative of seismic ground motions expected at the bridge location. In order to determine the characteristics of the seismic excitations, the seismic hazard for the bridge location was examined by Geological Survey of Canada based on the latest knowledge of the seismicity of the surrounding regions. The seismic hazard was represented by a uniform hazard spectrum, rather than by a spectrum based on peak ground motions and spectral amplification factors as used in the design of the bridge. Scenario earthquakes that have the largest contributions to the seismic hazard for the bridge location were also determined from the seismic hazard analysis.

For the purpose of the dynamic analysis of the bridge, a finite element model was developed using 3-D beam elements. The model consisted of a three-span segment of the

bridge that is representative of the entire bridge in terms of dynamic performance. Rotational springs in the longitudinal and transverse directions were introduced in the model, at the bases of the piers, to represent the foundation stiffness. The model was calibrated using measured data from static and dynamic tests of the bridge. The stiffness of the springs that provided a close match between the computed and measured data was used in the analyses.

A number of dynamic analyses were conducted by subjecting the model to selected seismic excitations representative of the expected seismic ground motions at the bridge location. The following seismic excitations were considered in the study: (i) excitations represented by the uniform hazard spectrum for the bridge location, (ii) ground motion records representative of seismic motions in eastern Canada, (iii) ground motion records representative of seismic motions from large earthquakes at large distances, (iv) records obtained during the 1988 Saguenay, Quebec earthquake, (v) records obtained during the 1982 Miramichi, New Brunswick earthquake, and (vi) simulated seismic ground motions for the bridge location. Simultaneous actions of horizontal and vertical excitations were used in the analyses.

The response parameters obtained from the seismic analyses included displacements, bending moments, axial forces, and shear forces. A detailed review of the response parameters showed that the displacements and the bending moments are quite sufficient for representing the seismic performance of the bridge. The seismic performance of the bridge was evaluated by comparing the maximum displacements and bending moments resulting from the dynamic analyses for the various seismic excitations with those obtained from the analysis of a model similar to that used in the design and subjected to seismic actions represented by the design spectrum.

6.2 Conclusions

The following are the main conclusions from this study:

(1) The foundation stiffness has significant effects on the natural periods of the bridge. The

periods for some modes of the model that included the foundation stiffness were approximately 12% longer than the periods of the model with fixed bases.

(2) The change of the modulus of elasticity of the concrete with the age of the concrete lead to notable variations in the dynamic performance of the bridge. The variations of the responses relative to the response values corresponding to the average modulus of elasticity of the concrete of E_c=40,000 MPa were found to be within the range of ±8.5%.

(3) The responses of the bridge for the excitation motions considered in this study were smaller than the estimated design values, with the exception of the responses from the seismic actions represented by the uniform hazard spectrum, which were somewhat larger than the design values.

(4) The seismic parameters used in the design of the bridge are representative of the expected seismic motions at the bridge location, and are quite appropriate for the required safety during the service life of the bridge.

6.3 Recommendation

In the dynamic analyses, the seismic excitations applied at the bases of piers were assumed to act simultaneously, i.e. the same motions were applied at each pier. However, since the spans are quite long (250 m each), it is believed that there would be some differences in the phases and the amplitudes of the seismic ground motions at different piers. Such differences can have significant effects on the dynamic performance of the bridge. An evaluation study should be conducted to investigate the performance of the bridge when subjected to multi-support seismic excitations.

References

Adams, J., and Halchuk, S. 2003. Fourth generation seismic hazard maps of Canada: Values for over 650 Canadian localities intended for the 2005 National Building Code of Canada. Open File 4459, Geological Survey of Canada, Ottawa, Ontario.

Adams, J., and Atkinson, G. 2003. Development of seismic hazard maps for the proposed 2005 edition of the National Building Code of Canada. Canadian Journal of Civil Engineering, 30: 255-271.

Atkinson, G.M., and Beresnev, I.A. 1998. Compatible ground-motion time histories for new national seismic hazard maps. Canadian Journal of Civil Engineering, 25: 305-318.

Brown, T.G., and Croasdale, K.R. 1997. Confederation Bridge ice force monitoring joint industry project annual report – 1997, IFN Engineering Ltd., Calgary, Alberta.

Computers and Structures Inc. 2000. SAP 2000 integrated software for structural analysis and design, Berkeley, California.

CSA. 1988. Design of highway bridges. Standard CAN/CSA-S6-88, Canadian Standards Association, Rexdale, Ontario.

Friberg, P., Rusby, R., Dentrichia, D., Johnson, D., Jacob, K., and Simpson, D. 1988. The M=6 Chicoutimi earthquake of November 25, 1988, in the province of Quebec, Canada. Preliminary NCEER strong motion data report, Lamont-Doherty Geological Observatory of Columbia University, Palisades, N.Y.

Ghali, A., Elbadry, M., and Megally, S. 2000. Two-year deflections of the Confederation Bridge. Canadian Journal of Civil Engineering, 27: 1139-1149.

Halchuk, S., and Adams, J. 2004. Deaggregation of seismic hazard for selected Canadian cities. Proceedings of the 13th World Conference on Earthquake Engineering, Vancouver, B.C., Canada, Paper No. 2470.

Heidebrecht, A.C., and Naumoski, N. 1986. The engineering characteristics of the 1982 Miramichi earthquake records. Proceedings of the Third U.S. National Conference on Earthquake Engineering, Charleston, South Carolina, Vol. 1, pp. 345-356.

Jaeger, L.G., Mufti, A.A., Tadros, G., and Wong, P. 1997. Seismic design for the Confederation Bridge. Canadian Journal of Civil Engineering, 24: 922-933.

JMS. 1996. Design criteria – Northumberland Strait Crossing Project. Revision 7.2. J. Muller International – Stanley Joint Venture Inc., San Diego, California.

Lau, D.T., Brown, T., Cheung, M.S., and Li, W.C. 2004. Dynamic modelling and behaviour of the Confederation Bridge. Canadian Journal of Civil Engineering, 31: 379-390.

Londono, N.A., Desjardins, S.L., and Lau, D.T. 2004. Use of stochastic subspace identification methods for post-disaster condition assessment of highway bridges. Proceedings of the 13th World Conference on Earthquake Engineering, Vancouver, B.C., Canada, Paper No. 2714.

MacGregor, J.G., Kenedy, D.J.L., Barlett, F.M., Chernenko, D., Maes, M.A., and Dunascegi, L. 1997. Design criteria and load and resistance factors for the Confederation Bridge. Canadian Journal of Civil Engineering, 24: 882-897.

MTO. 1991. Ontario highway bridge design code. Ministry of Transportation of Ontario, Downsview, Ontario.

Munro, P.S., and Weichert, D. 1989. The Saguenay earthquake of November 25, 1988 – Processed strong motion records. Open File Report No. 1966, Geological Survey of Canada, Energy, Mines and Resources, Ottawa, Ontario.

Naumoski, N., Heidebrecht, A.C., and Rutenberg, A.V. 1993. Representative ensembles of strong motion earthquake records. EERG Report 93-1, Earthquake Engineering Research Group, McMaster University, Hamilton, Ontario.

Naumoski, N., Tso, W.K., and Heidebrecht, A.C. 1988. A selection of representative strong motion earthquake records having different A/V ratios. EERG Report 88-01, Earthquake Engineering Research Group, McMaster University, Hamilton, Ontario.

Newmark, N.M., Blume, J.A., and Kapur, K.K. 1973. Seismic design spectra for nuclear power plants. Journal of the Power Division, Vol. 99, No. PO2, pp. 287-303.

Newmark, N.M., and Hall, W.J. 1982. Earthquake spectra and design. Monograph, Earthquake Engineering Research Institute, Berkeley, California.

Tadros, G. 1997. The Confederation Bridge: an overview. Canadian Journal of Civil Engineering, 24: 850-866.

Tremblay, R., and Atkinson, G.M. 2001. Comparative study of the inelastic seismic demand of eastern and western Canadian sites. Earthquake Spectra, Vol. 17, No. 2, pp. 333-358.

Weichert, D.H., Pomeroy, P.W., Munro, P.S., and Mork, P.N. 1982. Strong motion records from Miramichi, New Brunswick, 1982 aftershocks. Open File Report 82-31, Energy, Mines and Resources Canada, Ottawa, Ontario.